Tomas Bata University in Zlín
Faculty of Applied Informatics

Doctoral Thesis

Estimation of Material Permittivity in Free Space by Means of Inverse Problem Techniques

Řešení inverzního problému odhadu permitivity materiálu ve volném prostoru

Author:	**Ing. Pavel Tomášek**
Study program:	Engineering Informatics (P3902)
Branch of study:	Engineering Informatics (3902V023)
Supervisor:	doc. RNDr. Vojtěch Křesálek, CSc.
Opponents:	prof. RNDr. František Cvachovec, CSc.,
	prof. Ing. Rudolf Palenčár, CSc.,
	prof. RNDr. Ing. Miloš Šeda, Ph.D.

Zlín, July 2020

Key words: *backward reconstruction, complex permittivity, evolutionary algorithm, free space, inverse problem, optimization, scattering parameters, sensitivity analysis, uncertainty analysis*

Klíčová slova: *zpětná rekonstrukce, komplexní permitivita, evuluční algoritmus, volný prostor, inverzní problém, optimalizace, rozptylové parametry, citlivostní analýza, analýza nejistot*

ABSTRACT

The aim of the doctoral thesis is to design and implement a system for solving the inverse problem of estimation of electric permittivity of an unknown material or multiple layers of unknown materials. The proposed solution is based on the combination of an evolutionary algorithm and a direct mathematical model computing transmission and reflection coefficients of a defined material or a multi-layered structure of defined materials. Synthetic data as well as real data obtained by direct measurement of transmission and reflection coefficients in free space (frequency range: single units of gigahertz and higher) serve as the system input. Uncertainty and sensitivity analyses are also part of the study. Included experiments present reasonable estimations of complex permittivity with rather low uncertainties and low sensitivity on the error of the input data.

ABSTRAKT

Doktorská práce je zaměřena na návrh a implementaci systému řešícího inverzní problém určení elektrické permitivity neznámého materiálu či vrstev neznámých druhů materiálu. V navrženém řešení je využita kombinace evolučního algoritmu a přímého matematického modelu vypočítávajícího koeficienty odrazu a prostupu definovaného materiálu či vícevrstvé struktury definovaných materiálů. Vstupem systému jsou přitom právě koeficienty odrazu a prostupu ve volném prostoru ve frekvenčním rozsahu od jednotek gigahertz výše. V práci je též věnován prostor citlivostní analýze i analýze nejistot implementovaného sytému. Součástí práce jsou i experimenty jak se syntetickými daty, tak i s daty z přímých měření prokazující použitelnost navrženého systému. Odhady komplexní permitivity provedené v rámci experimentální části jsou uspokojivé, s poměrně nízkou mírou nejistot a současně s přijatelnou tolerancí vůči úrovni chyby u vstupních dat.

TABLE OF CONTENTS

LIST OF FIGURES

LIST OF TABLES

LIST OF ABBREVIATIONS

C-Band	The electromagnetic spectrum from 4 to 8 GHz
CFC	Carbon Fiber Composite
CPU	Central Processing Unit
DE	Differential Evolution
EA	Evolutionary Algorithm
ES	Evolution Strategies
FR	Flame Retardant
GA	Genetic Algorithm
GNU	GNU is Not Unix
GPL	General Public Licence
MOP	Multi-Objective Optimization Problem
PMMA	Poly-Methyl-Methacrylate
POPOT	POPulation based Optimization Toolbox
PRNG	Pseudorandom Number Generator
PTFE	Polytetrafluoroethylene
RF	Radio Frequency, from 3 kHz to 300 GHz
RMS	Root Mean Square
RSD	Relative Standard Deviation
S-Parameters	Scattering Parameters
SI	International System of Units
SOMA	Self-Organizing Migrating Algorithm
VNA	Vector Network Analyser
V-Band	The electromagnetic spectrum from 40 to 75 GHz
W-Band	The electromagnetic spectrum from 75 to 110 GHz
X-Band	The electromagnetic spectrum from 8 to 12 GHz

1   INTRODUCTION

The importance of material properties awareness is rising. In the last few decades, new artificial materials have been developed, but in most cases, their properties have not yet been fully described. This lack of knowledge and the need to enable people to work with these new types of materials give scientists the opportunity to bridge this significant gap.

The aim of this doctoral thesis was to find a solution – or rather one of possible ways – to estimate electromagnetic properties of an unknown material or several unknown materials in a layered structure.

This doctoral thesis describes the process of design of a new system estimating complex permittivity of a single or multi-layered structures of non-magnetic homogeneous isotropic materials of known thicknesses. The aim of this work is also to develop a software tool implementing the theoretical system in order to help scientists and material engineers to estimate properties of unknown materials. The number of such materials has grown in the last decade. This is mainly due to numerous modern nanomaterials, polymers and composites. These materials are usually produced with limited information related to their properties, such as complex permittivity (moreover, in higher frequencies corresponding to sub-millimeter waves).

The project presented in this thesis is based on synthetic as well as measured transmission coefficients in free space of a single material or multi-layered structures of different materials. Measurements in free space have been selected so as to enable measuring transmission coefficients even in very high frequencies (up to single units and tens of terahertz). The measured parameters are processed in a system for backward reconstruction of permittivity employing an evolutionary algorithm. This process is described in more detail below.

The presented system for backward reconstruction of complex permittivity has been tested using synthetic data as well as using noisy synthetic data and real (measured) data. The results of these experiments, including uncertainties, are also part of the thesis.

1.1 Thesis Structure

The thesis consists of the introduction to this specific area (section 1), which is followed by the research aims and objectives explaining also why this topic can be considered trendy and relevant for the contemporary world (section 2) and by the description of the state of the art, including literature overview (section 3).

The following sections are devoted to the introduction and utilization of the evolutionary algorithms (section 4), description of applied methods and technologies in more detail (section 5), various experiments with synthetic data, noisy synthetic data and with data obtained by direct measurement (section 6), uncertainty and sensitivity analysis of the complex software solution (section 7).

The conclusion of the thesis consists of its summary, contributions and tips for possible future work (section 8), references, list of the author's scientific publications, his curriculum vitae and, last but not least, appendices.

2 RESEARCH AIMS AND OBJECTIVES

Nowadays the boom of development of new artificial materials (like various kinds of composites, polymers and nanomaterials) is so great that developers, constructors, engineers, physicists, chemists and scientists in general can select from an enormous spectrum of materials and ways of how to compile their design, construction or product. The utilization could be much wider if there was information about all properties of such materials. This study is going to help to define one specific property: the complex permittivity.

This work is aimed at help in estimation of the permittivity of unknown nonmagnetic homogeneous isotropic materials. Therefore, the most applicable general idea (i.e., the problem) is that there is an unknown material and there is a need to define it (or at least its properties). This is the direct application of the system developed in the doctoral thesis. The submission is wide and the doctoral thesis may be designated as multidisciplinary because of its relations

with the areas of material science, mathematics, applied information technology and measurement.

The objectives of this thesis can be summarised into the following list:

- synthesis of a direct mathematical model computing reliable S-parameters (transmission and reflection coefficients) of a layer of a defined material as well as of a multi-layered structure of defined materials in free space at certain frequency range, where the materials are non-magnetic homogeneous isotropic,

- implementation of the direct model into a software,

- verification of the direct model by comparing its computed synthetic data with data obtained by direct measurements,

- implementation of an evolutionary algorithm into the software and combining it with the direct model,

- experimental part: confrontation of the permittivities of known standard materials with the permittivities estimated by the developed system using synthetic S-parameters as well as S-parameters obtained by direct measurements, and

- elaboration of the uncertainty and sensitivity analysis of the final system.

3   STATE OF THE ART

Basic theoretical fundamentals of this work including the relation among the electric complex permittivity of a material, its thickness, the transmission and reflection coefficients is mentioned in this section.

The problem of propagation of incident waves through several layers is frequently mentioned in the available scientific literature. Thus also this may be considered as an indication for an important area.

The theoretical fundamentals of dielectric properties including electric permittivity mentioned in the section below are mainly based on the knowledge presented in *Encyclopedia of RF and Microwave Engineering* [37], *Fundamentals of Physics* [28], *Industrial Microwave Heating* [41] and *The electromagnetic properties of food materials: A review of the basic principles* [55].

Furthermore, significant information related to the ways of computation of the transmission and reflection coefficients are presented in research denoted to a quasi-optical free space measurement setup without time domain gating for material [10], a free-space measurement of complex permittivity and complex permeability of magnetic materials at microwave frequencies [25], a design of broadband radar absorbing materials for large angles of incidence [49], a free-space method for measurement of complex permittivity of silicon wafers at microwave frequencies [5], an improved technique for determining complex permittivity with the transmission/reflection method [6], a free-space method for measurement of complex permittivity of double-layer dielectric materials at microwave frequencies [66], a development of the complex permittivity measurement system for high-loss biological samples using the free space method in quasi-millimeter, and millimeter wave band [56], determination of permittivity and dissipation factor of thin layers in microwave range of electromagnetic spectra in free space employing evolutionary algorithms [36], and finally the estimation of material properties in free space [31].

3.1 Related Work

The contemporary scientific literature provides many articles related to the goals of this work. The following research contains some further information which was helpful while orienting in the area of estimation of the material properties of unknown materials. It was a research aimed at a broadband free-space dielectric properties measurement system at millimeter wavelengths [22], material characterization using a quasi-optical measurement system introducing also calibration and correction methods of quasi-optical system [23], timed domain free-field measurements of the relative permittivity of building materials [26], a study on

measurement of dielectric constant by free space transmission method at C-Band [29], a simple free space method for measuring the complex permittivity of single and compound dielectric materials [38], compact unfocused antenna setup for X-Band free space dielectric measurements based on Line-Network-Network calibration method [45], a free space measurement technique on dielectric properties of agricultural residues at microwave frequencies [64] and a quasi-optical free space method for dielectric constant characterization of polymer materials in mm-wave band [18]. And the last group of useful papers follows. It was the research denoted to W-Band free space permittivity measurement setup for candidate radome materials [21], dielectric permittivity measurement methods of textile substrate of textile transmission lines [39], an improved calibration technique for free-space measurement of complex permittivity [43] and complex permittivity measurements of common plastics over variable temperatures [53].

3.2   Complex Electric Permittivity

Electric permittivity is a constant of proportionality (in a closed frequency range) that exists between electric displacement field D and electric field intensity E (in free space):

$$\epsilon = \frac{D}{E} \tag{3.1}$$

Permittivity divided by permittivity of vacuum (a constant, $\epsilon_0 = 8.8542 \ pF/m$ approx. [28]) is called relative permittivity (relative to the vacuum):

$$\epsilon_r = \frac{\epsilon}{\epsilon_0} \tag{3.2}$$

Relative permittivity of an isotropic dielectric is a scalar constant considering usual (low) frequency ranges. This assumption may not be true when considering wide ranges of frequencies from units of GHz to units or tens of THz.

There is a variety of definitions of permittivity in the literature. The definitions usually differs only due to the area of focus. Therefore, one definition states that the value of relative permittivity of a material indicates how much increases the

Tab. 3.1 Relative permittivity
of several dielectrics (under
general conditions, 20 °C) [28]

Material	ϵ_r
Air	1.00054
Polystyrene	2.6
Paper	3.5
Pyrex	4.7
Mica	5.4
Porcelain	6.5
Silicon	12
Ethanol	25
Water	80.4

capacity of a capacitor when using this material in between the electrodes of the capacitor [28]. In another definition reader finds permittivity as a quantity used to describe dielectric properties that influence reflection of electromagnetic waves at interfaces and the attenuation of wave energy within materials [37].

Tab. 3.1 informs about typical relative permittivity of general materials like air, paper and water.

In frequency domain, the complex relative permittivity ϵ_r^* of a material can be expressed in the following form [25]:

$$\epsilon_r^* = \epsilon_r' - j\epsilon_r'' \tag{3.3}$$

The real part ϵ_r' is referred to as the dielectric constant and represents stored energy when the material is exposed to an electric field, while the dielectric loss factor ϵ_r'', which is the imaginary part, influences energy absorption and attenuation [37], and

$$j = \sqrt{-1} \tag{3.4}$$

Another important parameter used in electromagnetic theory is a tangent of loss angle [37]:

$$tan(\delta) = \frac{\epsilon_r''}{\epsilon_r'} \tag{3.5}$$

Therefore, complex relative permittivity ϵ_r^* can be also defined as:

$$\epsilon_r^* = \epsilon_r' \left(1 - jtan(\delta)\right)$$ (3.6)

Mechanisms that contribute to the dielectric loss in heterogeneous mixtures include polar, electronic, atomic, and Maxwell–Wagner responses [41]. At RF and microwave frequencies of practical importance and currently used for applications in material processing, ionic conduction and dipole rotation are dominant loss mechanisms [55]:

$$\epsilon_r'' = \epsilon_d'' + \epsilon_\sigma'' = \epsilon_d'' + \frac{\sigma}{\epsilon_0 \omega}$$ (3.7)

where subscripts d and σ stand for contributions due to dipole rotation and ionic conduction, respectively; σ is the ionic conductivity in S/m of a material, ω is the angular frequency in rad/s [37]:

$$\omega = 2\pi f$$ (3.8)

where f stands for frequency.

Penetration depth of microwave and RF power is defined as the depth where the power is reduced to $1/e$ (where $e = 2.718$) of the power entering the surface (see Fig. 3.1). The penetration depth d_p in meters of RF and microwave energy in a lossy material can be calculated by [60]:

$$d_p = \frac{c}{2\pi f \sqrt{2\epsilon' \left[\sqrt{1 + \left(\frac{\epsilon''}{\epsilon'}\right)^2} - 1\right]}}$$ (3.9)

where c is the speed of light in vacuum ($299\,792\,458\ m/s$ [57]).

Dielectric lossy materials convert electric energy at RF and microwave frequencies into heat. Given fixed dielectric properties, the penetration depth of a material is inversely proportional to frequency. It is; therefore, expected that in general deeper penetration corresponds to lower frequencies, and that higher frequencies result in greater surface heating [37].
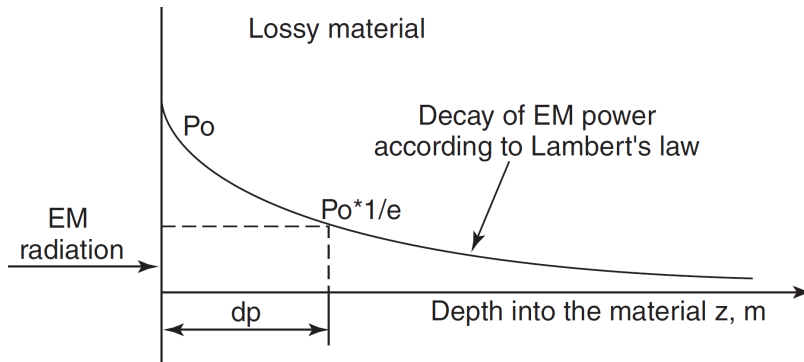
Fig. 3.1 Typical penetration depth inside a large-sized material
(larger than the wavelength) [37]

3.3 Computation of Transmission and Reflection Coefficients

Correct valid theory must be placed and implemented while thinking about using
a direct model computing transmission/reflection coefficients. Therefore, some
fundamental equations derived from Maxwell's theory are presented below to
reveal the computational mechanism. Only perfect mathematical model can be
joined with an evolutionary algorithm and thus assure acceptable estimations of
complex permittivities of materials.

The list of input data to the direct model follows (considering a single material
or a multi-layered structure of materials under test):

- number of layers,

- relative permittivity of each layer,

- thickness of each layer,

- angle of incidence, and

- set of frequencies.

A possible multi-layered structure is visualised in Fig. 3.2. There are three
sections of materials in this illustration. The first and the third layers are of the
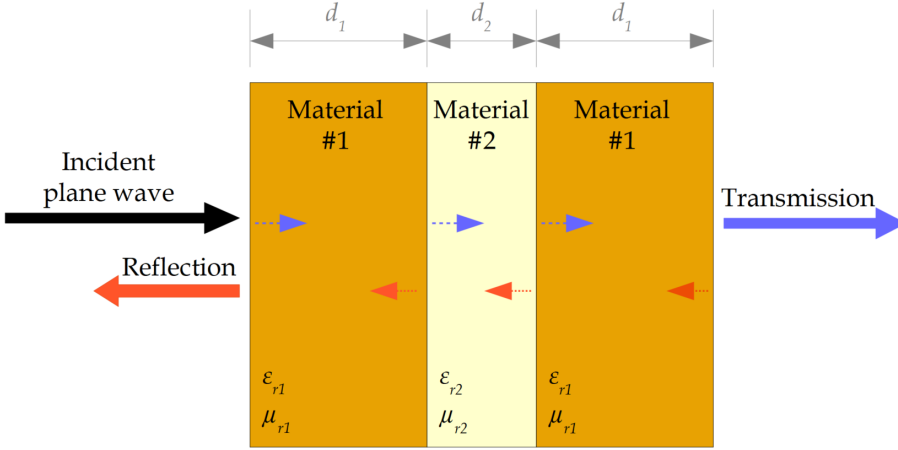
Fig. 3.2 Schema of a sandwich structure of materials under test,
side view, incident plane waves come from the left, S_{11} represents
the reflection and S_{21} is the transmission on these materials

same material #1 with the same thickness (d_1). The incident plane waves come
perpendicularly (the angle of incidence $\Theta = 0$). This sandwich structure may be
also used to estimate properties of some liquid as material #2.

The contemporary literature is saturated with mathematical descriptions of
propagation through materials of known properties. Fundamental theory and
equations based on previous research [10, 25, 49, 36] with its further explanation
follows:

$$\sigma = -\epsilon'_r \, \epsilon_0 \, \omega \, tan(\delta) \tag{3.10}$$

$$Z_{m-1} = K_{m-1} \frac{Z_m + K_{m-1} \tanh(U_{m-1} d_{m-1})}{K_{m-1} + Z_m \tanh(U_{m-1} d_{m-1})} \tag{3.11}$$

$$\gamma_m^2 = -\mu_m \, \epsilon_{rm} \, \epsilon_0 \, \omega^2 + j \, \sigma_m \, \mu_{rm} \, \mu_0 \, \omega \tag{3.12}$$

$$L = j \, \gamma_0 \, sin(\Theta) \tag{3.13}$$

$$U_m = \sqrt{L^2 + \gamma_m^2} \tag{3.14}$$

$$K_0 = \sqrt{\frac{\mu_0}{\epsilon_0}} \, cos(\Theta) \tag{3.15}$$

$$K_m = \frac{U_m}{\sigma_m + j \, \omega \, \epsilon_{rm} \, \epsilon_0} \tag{3.16}$$

$$R_0 \quad = \quad \frac{K_0 - Z_1}{K_0 + Z_1} \tag{3.17}$$

R_0 represents the desired reflection coefficients on the layered media related to the specific frequency f (and corresponding angular frequency ω). Each layer of a material (subscript $_m$) is represented by complex relative permittivity $\epsilon'_{rm} - j\epsilon''_{rm}$, relative permeability μ_{rm}, thickness d_m, conductivity σ_m, loss tangent $\tan \delta_m$, wave impedance Z_m, wave impedance of the incidence region K_m (whereas Θ stands for the angle of incidence) and, finally, propagation constant U_m.

There is a free space before and after the layered structure under test (this thesis is aimed at free space measurements). Therefore, the wave impedance of the last layer is given by $Z_n = K_0$ (where n is equal to the number of layers).

The values of R_0 are absolute values (not logarithmic) of the closed interval of $[0.0, 1.0]$.

4 EVOLUTIONARY ALGORITHMS

This section presents a brief introduction into the field of evolutionary algorithms (EAs) enumerating also several major representatives. This section is closed by a focus on the problem solved in this doctoral thesis with explanation of how an EA is used for the backward reconstruction.

EAs belong to the area of artificial intelligence. They are stochastic population-based metaheuristic algorithms. Such algorithms are used in single-objective (or more often) in multi-objective optimization problems (MOPs) [13].

The rising interest in EAs in the last decades is based on the capability of solving complex problems. There is a wide usage of EAs in the area of optimization and classification. The EAs are usually inspired by nature what can be recognized in the names of the most used kinds of these algorithms and their internal operators and structures.

In the 1950s and the 1960s several computer scientists independently studied

Tab. 4.1 General terminology in the field of EAs [32]

Term	Description
Individual/Particle	A representative of one particular solution (one hypothesis)
Population	A set of trial solutions
Parent	A member of the current generation
Child/Offspring	A member of the next generation
Generation	Successively created populations (iterations)
Chromosome	The coded form of a trial solution vector (string) consisting of genes made of alleles
Fitness/Cost	Positive number assigned to an individual representing a measure of goodness, it is computed by a fitness/cost/objective function

evolutionary systems with the idea that evolution could be used as an optimization tool for engineering problems. The idea in all these systems was to evolve a population of candidate solutions to a given problem, using operators inspired by natural genetic variation and natural selection [42].

4.1   Terminology and Elements of Evolutionary Algorithms

The general terminology used in EAs is described in Tab. 4.1. In general, a representative of the group of EAs performs a defined sequence of steps. The workflow of the Genetic Algorithms is for instance depicted in Fig. 4.1. There is a conditional test and three specific operators in each iteration of the algorithm: *selection*, *crossover*, and *mutation*. Selection operator defines how to choose the individuals in the population that will create an offspring for the next generation, and how many offspring will each create. The purpose of selection is, of course, to emphasize the fitter individuals in the population in hopes that their offspring will in turn have even higher fitness. Selection has to be balanced with variation from crossover and mutation. Furthermore, crossover is one of the distinguishing features of Genetic Algorithms. It can be a single−point or a two-point crossover. Crossover with mutation are the major instruments of variation and innovation insuring the population against permanent fixation at any particular focus [42].
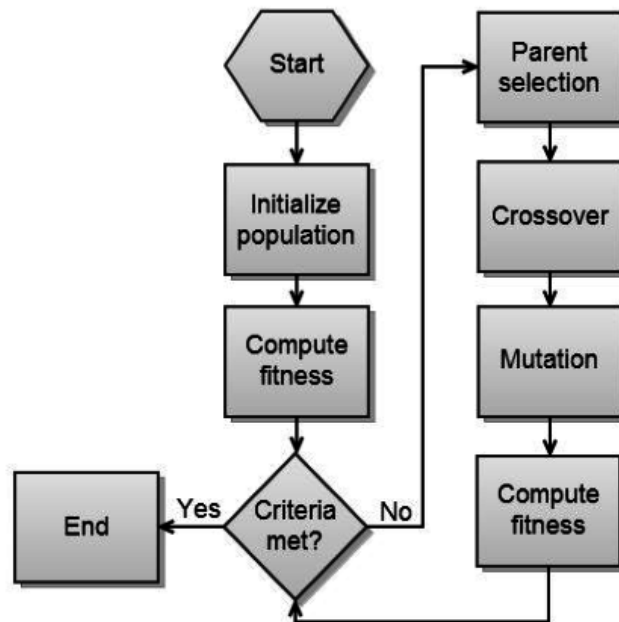
Fig. 4.1 Simplified Genetic Algorithm workflow [9]

A problem to be solved in an EA has to be mathematically explicitly expressed. Afterwards, such an expression is used in so called *fitness function*. There are variants of the name of this function in contemporary literature. It can be also labelled as *criterial* or *cost function*. The function is responsible for evaluation of individuals. Examples of such functions are presented in subsection 4.3. The fitness is computed for all the individuals in each iteration of an EA. Consequently, the fitness value plays a significant role in the process of creating a new generation. This process vary throughout the EAs.

4.2 Representatives of the Group of Evolutionary Algorithms

Common representatives of the EAs are

- Evolution Strategies,

- Genetic Algorithms,

- Genetic Programming,

- Scatter Search,

- Differential Evolution,

- Bees Algorithm,

- Cuckoo Search,

- Ant Colony Optimization,

- Particle Swarm Optimization, and

- Self-Organizing Migrating Algorithm.

Several EAs are briefly described below.

4.2.1 Evolution Strategies

Evolution Strategies (ES) started in the past with a "population" of only two individuals, one parent and one offspring, the offspring being a mutated version of the parent; neither crossover nor mutation were incorporated in the first version of this technique. The selection is only made by the fitness value; therefore, in a deterministic way [42].

4.2.2 Genetic Algorithms and Genetic Programming

Genetic Algorithms (GAs) were invented by John Holland in the 1960s and were developed by Holland and his students and colleagues at the University of Michigan. In contrast with Evolution Strategies and Evolutionary Programming, Holland's original goal was not to design algorithms to solve specific problems but rather to formally study the phenomenon of adaptation as it occurs in nature and he also wanted to develop ways in which the mechanisms of natural adaptation might be imported into computer systems [42].

The workflow and internal operators have been already generally described in subsection 4.1.

Related Genetic Programming represents another variant of the group of EAa which is based on the idea of Genetic Algorithms focused on optimizing a source code of a software planned to perform some specific activity.

4.2.3   Differential Evolution

Differential Evolution (DE) was created in the mid-1990s. It was proposed by Kenneth Price and Rainer Storn. DE was designed to optimize problems over continuous domains [44].

This approach originated from Price's attempts to solve the Tchebycheff Polynomial fitting problem that had been posed to him by Storn. In one of the different attempts to solve this problem, Price came up with the idea of using vector differences for perturbing the vector population [44].

Fig. 4.2 illustrates the mechanism of creation of an individual from parents of a current generation. The weighted differential vector of a randomly selected individuals is applied on another individual. Such a new position is accepted if it represents an improvement.

4.2.4   Self-Organizing Migrating Algorithm

Self-Organizing Migrating Algorithm (SOMA) is a modern method which was published by Ivan Zelinka in the year of 2000 [67]. The process of creation of a new generation is substituted for so-called migration loops. The process of creation of a new individual is depicted in Fig. 4.3. All the possible positions of a new individual are calculated before its creation using multiplications of ordinal numbers with a defined length of step and differential direction.
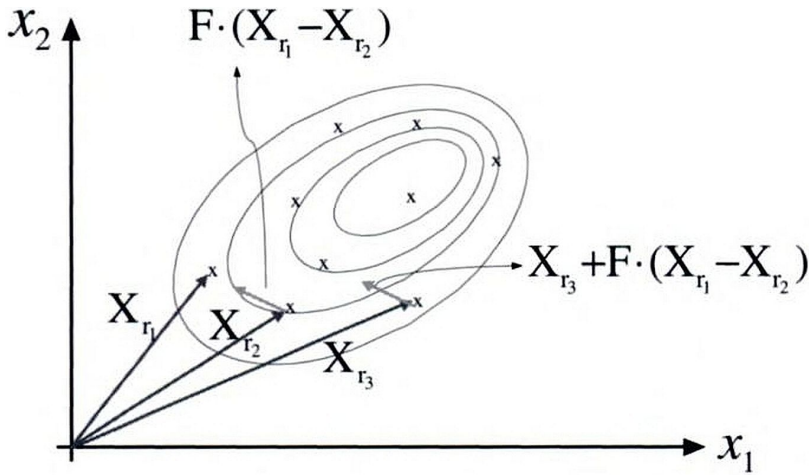
Fig. 4.2 Creation of a new individual in DE. Three vectors $X_{r1..r3}$ represent three randomly selected individuals from a generation. $F(X_{r1} - X_{r2})$ is a weighted difference between the first two individuals. Finally, $X_{r3} + F(X_{r1} - X_{r2})$ defines the offspring [44].
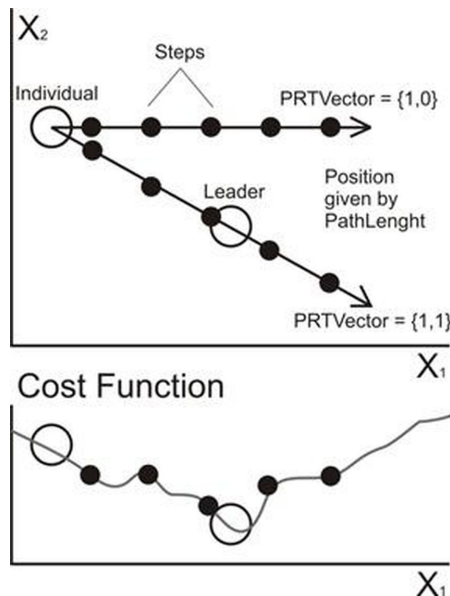
Fig. 4.3 Creation of a new individual in SOMA. The third position (black point) is evaluated as the best choice in this example due to the lowest fitness [30].

4.2.5   Particle Swarm Optimization

Particle Swarm Optimization (PSO) is a parallel EA. PSO is based on swarm, which was proposed by Eberhart and Kennedy in 1995 [35]. PSO algorithm simulates animal's social behaviour, including insects, herds, birds and fishes. These swarms conform a cooperative way to find food, and each member in the swarms keeps changing the search pattern according to the learning experiences of its own as well as of the other members.

Creation of a new individual (called a particle) in Particle Swarm Optimization is based on several aspects. It is the own confidence of the particle (its own memory and its own vector of velocity) and also the information about the best position found by the whole swarm. Fig. 4.4 illustrates the movement of a particle.

PSO's advantages can be summarized as follows: its convergence rate is fast without the need of prefect set up of its control parameters; the algorithm is simple, robust and easy to implement [62].
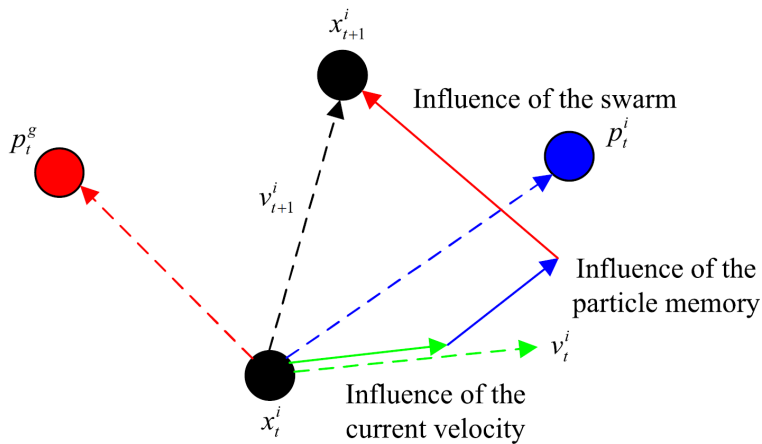
Fig. 4.4 Creation of a new particle in PSO [62]

4.3   Benchmark Problems

Benchmark problems are special single or multi-objective test problems which are prepared in order to sort the selected solvers with emphasis on desired aspects.

The benchmarks used in the field of EAs usually test the robustness and speed of convergence of a particular EA what means whether the technique is able to converge and find the global optimum in a finite time.

Rastrigin's function is a typical example of such a benchmark problem. Other typical MOPs are Schaffer's, Fonseca's, Kursawe's, Poloni's or Ackley's functions [13]. Ackley's and Rastrigin's functions have been selected as typical representatives for further presentation in this subsection.

4.3.1 Ackley's Function

Ackley's function is a continuous and multi-modal test function obtained by modulating an exponential function with a cosine wave of moderate amplitude. Its topology is characterized by an almost flat outer region and a central hole or peak where modulations by cosine wave become more and more influential. Visualization of a 3-dimensional variant is depicted in Fig. 4.5. Ackley's function's definition follows:

$$f(x_1, .., x_n) = -a \exp\left[-b\sqrt{\frac{1}{n}\sum_{i=1}^{n}x_i^2}\right] - \exp\left[\frac{1}{n}\sum_{i=1}^{n}cos(cx_i)\right] + a + \exp(1) \quad (4.1)$$

where the usual setup of constants is $a = 20$, $b = 0.2$, $c = 2\pi$ and n defines the number of dimensions [27]. Its global minimum is $f(0, .., 0) = 0.0$.

4.3.2 Rastrigin's Function

Rastrigin's function is highly multimodal. It generates numerous local minima. This function represents a difficult MOP. Therefore, this functions with its variations serve as a common benchmark for EAs. Visualization of a 3-dimensional variant is depicted in Fig. 4.6 and Fig. 4.7. Rastrigin's function has the following definition:

$$f(x_1, .., x_n) = 10n + \sum_{i=1}^{n}\left[x_i^2 - 10cos(2\pi x_i)\right] \quad (4.2)$$

where n defines the number of dimensions of the problem. Test area is usually
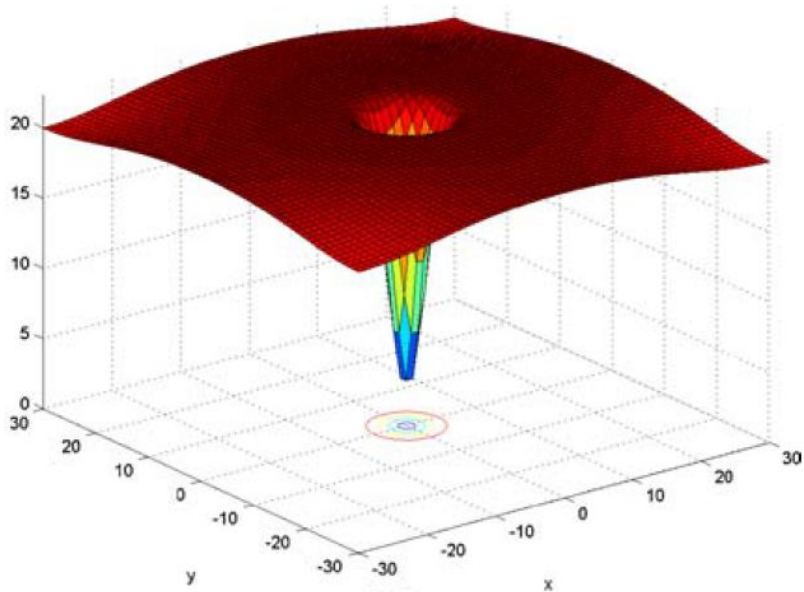
(a)
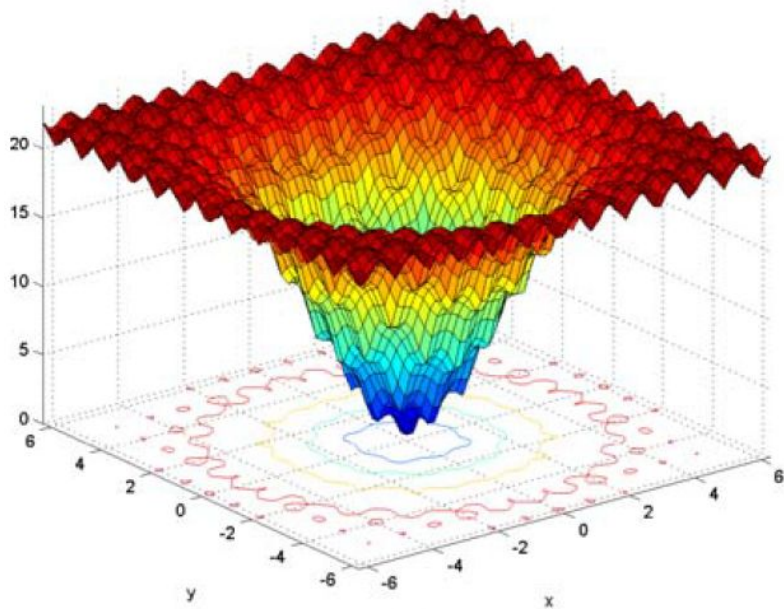
(b)

Fig. 4.5 3D Ackley's MOP for (a) $-30 \leq x_{1,2} \leq 30$ and (b) $-6 \leq x_{1,2} \leq 6$ [27]
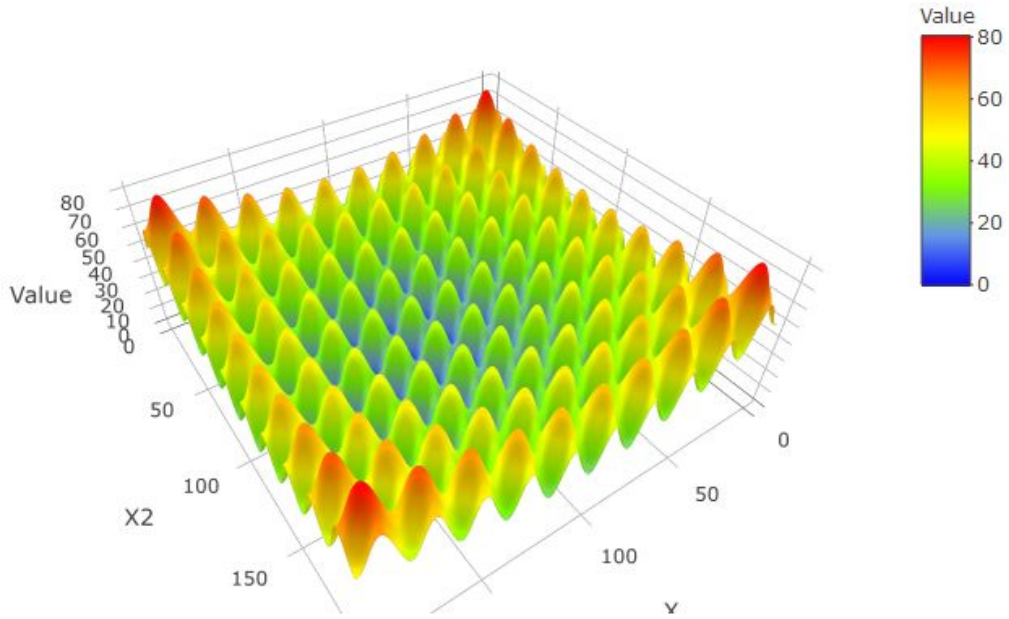
Fig. 4.6 3D Rastrigin's MOP [11]
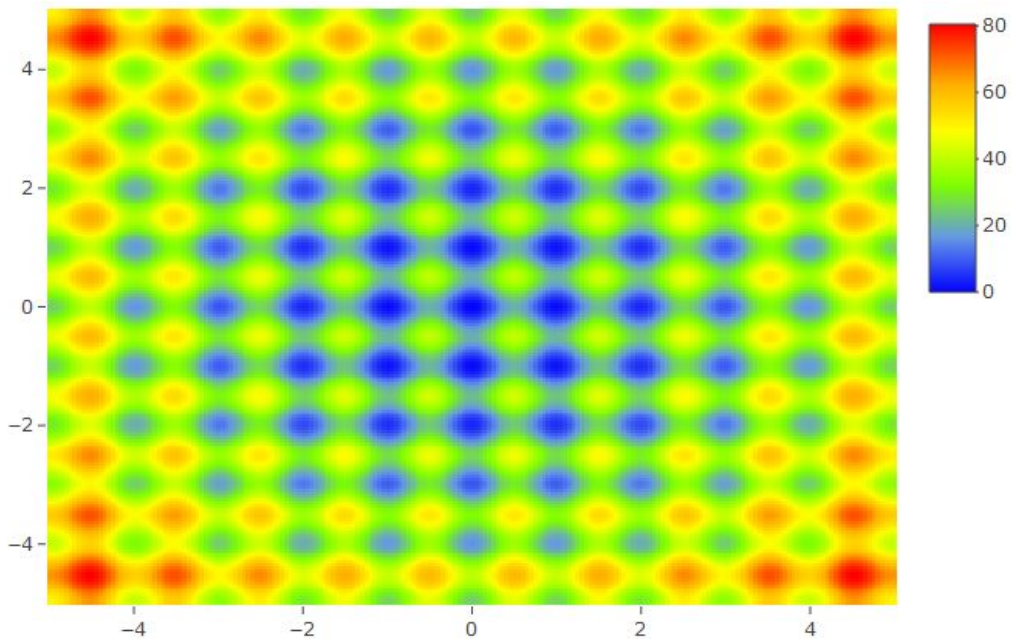
Fig. 4.7 3D Rastrigin's MOP mapped into 2D [11]

restricted to a hypercube $-5.12 \leq x_{i..n} \leq 5.12$ [65]. Its global minimum is $f(0,..,0) = 0.0$.

4.4 Utilization of an EA in the Doctoral Thesis

Mentioning the situation to be solved in this doctoral thesis, the estimation of permittivity of unknown materials, each layer in multi-layered structures under test is represented by two unknowns. They are the real and the imaginary part of the desired complex relative permittivity. Therefore, having one, two, three or more-layered structure under test means also having two, four, six or generally $2n$-dimensional MOP where n stands for the number of layers in the structure under test.

It is obvious that having multi-layered structures of unknown materials under test makes the task of estimation of permittivities very difficult. In these circumstances an EA have been selected as a theoretically suitable solver.

This doctoral thesis is not aimed at analysis and comparison of multiple evolutionary algorithms presenting their capabilities or differences. This topic is covered by available literature (for instance [13]). Particle Swarm Optimization has been directly selected for incorporation in the developed system. This choice is based on the author's previous research and experiences in the area of inverse processing. Particle Swarm Optimization is robust and fast enough. It does not require special configuration and enables setting of intervals for each design parameter. A competitive modern method of Self-Organizing Migrating Algorithm has not been used there due to higher sensitivity on the setup of its control parameters (based on the author's empirical testing in the past).

Generally, EAs are non-deterministic and may suffer from getting stuck in some local optimum and thus not finding the global one (that is also one of the reasons for testing the EAs on the benchmark MOPs). Another potential disadvantage of using these algorithms is that they can reveal more acceptable solutions which can perfectly suit (theoretically) but their practical meaning may be considered as a nonsense (like having a negative permittivity while not working with meta-

materials etc.). This can be partially bypassed by using appropriate lower and
upper bounds of the expected permittivity for which the algorithm is looking
for.

5   METHODOLOGY

This section contains an overview of the methods, main technologies and ap-
proaches used in this doctoral thesis aimed at estimation of complex permit-
tivities of single or multi-layered structures. The following subsections includes
a brief description of the applied scientific methods, the way of data acquisi-
tion (S-parameters) and its further post-processing techniques implementing a
mathematical model combined with a specific EA in a preferred programming
language.

5.1   Applied Scientific Methods

The list of scientific methods which have been employed in this work follows.
Procedures are rather theoretical at the beginning and practical at the end of
the following list:

- analysis of the state of the art related to the electric permittivity, S-
  parameters and EAs,

- hypothesis about development of a new way of complex permittivity esti-
  mation based on backward reconstruction using measured S-parameters,

- synthesis of a direct mathematical model capable of computing reliable
  S-parameters of a given single material or a multi-layered structure,

- synthesis of the direct model and an EA into a software instrument using
  a programming technology,

- experiments with the result of the previous step, estimation of permittivity
  using the EA employing the direct model on data synthesized by the direct

model itself,

- comparisons of the output of the experiments from the previous step with the expected permittivities of the original materials (and thus verifying the implementation of the combination of the direct model and the evolutionary algorithm),

- experiments with real known materials, measurement of their S-parameters and estimating their permittivities using the developed software instrument afterwards,

- comparisons of the estimated permittivities of materials in the previous experiment with their real (expected) permittivities,

- repetitions of the previous experiments & results comparisons and also experimenting with different materials (various experimental setups),

- analysis of sensitivity of the software instrument on the input error level, and

- analysis of uncertainties of the output of the software instrument in various experimental setups.

5.2 Measurements in Free Space Employing VNAs

As presented in the State of the art (section 3), the way of measurement of S-parameters is already known. What is unknown and non-trivial is the utilization of the system as a source of information for processing and estimation of permittivity of a sample of an unknown material. And this approach is briefly described in this section.

Fig. 5.1 shows the basic electromagnetic spectrum. The interest of this work is situated in the area of microwaves what means the range from units to hundreds of GHz approximately with respect to the frequency.

There is one insuperable reason for measuring in free space against the measurement using a waveguide. The reason relates to the frequency range of interest.
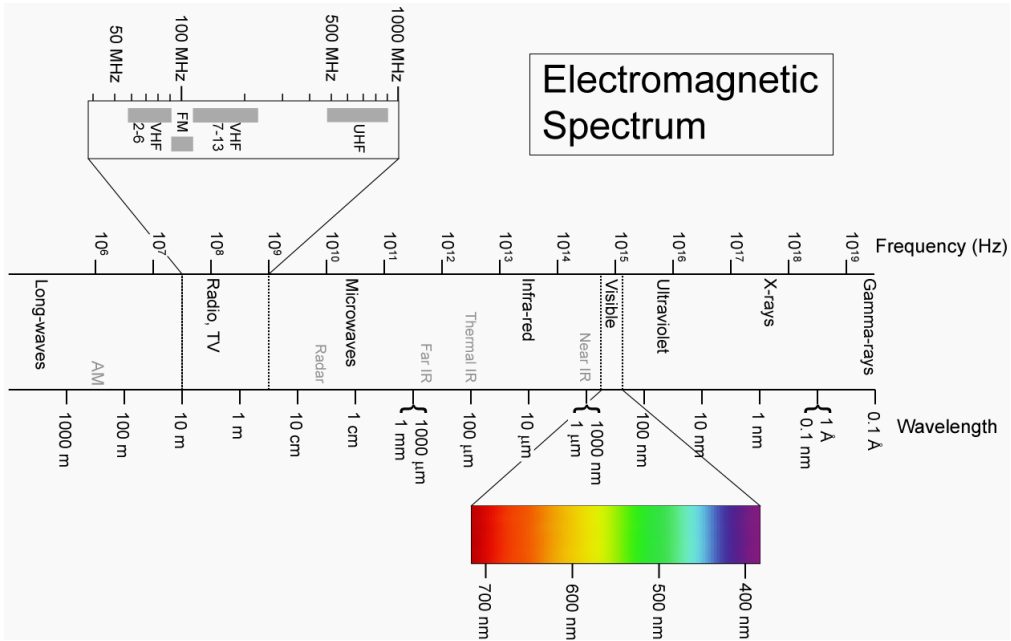
Fig. 5.1 Illustration of the electromagnetic spectrum [34]

It is planned to work with frequencies higher than units of GHz. Dimensions of a typical waveguide for such a task are too low. Common rectangular waveguides for V-Band: R620 (frequency band of operation: 50.00 GHz – 75.00 GHz; cutoff frequency of lowest order mode is at 39.875 GHz; cutoff frequency of the next mode is at 79.750 GHz) have inner dimensions 3.759 mm × 1.880 mm approximately (0.148 inch × 0.074 inch) [19]. These sizes are too low and become even lower with higher frequencies. Fig. 6.9 shows a common waveguide measurement for illustration. Therefore, the limitations in dimensions does not allow to work with waveguides at the planned range of frequencies.

A material under test must be placed between the sending and receiving horn antennas. The information from the antennas (reflection and transmission coefficients, S_{11} and S_{21} respectively) is then captured by a calibrated vector network analyser (VNA). The general schema of planned experimental setup is presented in Fig. 5.2.

The possibility of testing of liquids is also open. This supposes some kind of
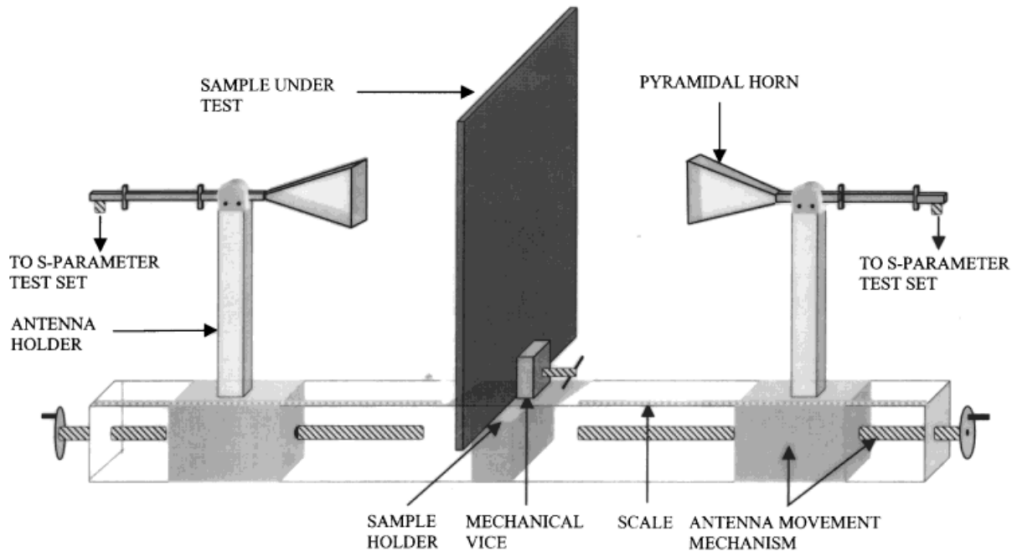
Fig. 5.2 Schema of a test bench with a sample in free space [38]

a sandwich structure (a box) as a holder. Such a structure could consist of a two layers of material of well known properties (like polytetrafluoroethylene with known thickness and complex permittivity) holding the material under test in a box. This sandwich structure is presented in Fig. 3.2.

5.3 Software for S-Parameters Post-Processing

The software post-processing the measured S-parameters has been written in C++ programming language. The reason for this choice is the efficiency and speed of the software written in this language, simple portability between different architectures and operating systems. C++ is a modern, object-oriented and also performance-oriented programming language. The name of this language has appeared in 1983 for the first time and despite its age it is still modern and preferred language not only in low-level highly effective programming. Its current standard comes from 2017 (usually marked as C++17) and a fresh C++20 is coming soon [58]. The final software runs in a command-line/terminal environment with possibility of running with parameters what represents more robust approach in the point of view of automatized sequential as well as parallel

launching in a batch.

The Particle Swarm Optimization is the preferred EA which has been imple-
mented in the final software. This choice has been commented in the section
of Evolutionary Algorithms (section 4). Shortly, the reason of such a choice is
represented by the main advantages of this EA (in comparison with the other
common EAs):

- the ability of finding global optimum also in very difficult multi-objective
  problems (Rastrigin's MOP for instance, described in subsection 4.3.2),

- the speed of convergence, and

- PSO is not very sensitive on the settings of the control parameters (the
  number of individuals and the length of a step for example).

Framework called *Population based Optimization Toolbox* (POPOT) written in
C++ is used as the working implementation of PSO. This framework has been
published under GNU General Public Licence (GPL) version 3 [20] and thus it
is legal to use it freely in this doctoral thesis.

Each particle in the PSO represents an individual solution of the problem. There-
fore each particle is defined by values of real and imaginary parts of the complex
relative permittivities of all the materials in the layered structure under test.
This means that it is possible to compute S-parameters using any particle in the
population.

The fitness function is performing evaluation of each particle. Such an evalua-
tion is represented by computing the norm of the vector defined by position of
given and computed complex S-parameters. This is generalized in the following
formula:

$$
\begin{aligned}
f_p^2 = &(S_{g1\_real} - S_{c1\_real})^2 + (S_{g1\_imag} - S_{c1\_imag})^2 \\
&+ (S_{g2\_real} - S_{c2\_real})^2 + (S_{g2\_imag} - S_{c2\_imag})^2 \\
&+ \dots \\
&+ (S_{gn\_real} - S_{cn\_real})^2 + (S_{gn\_imag} - S_{cn\_imag})^2
\end{aligned}
\tag{5.1}
$$

where f_p stands for the fitness of a particular particle p, S_{gi} is the given i-th S-parameter (from an input file containing measured or synthetic data), S_{ci} is the computed i-th S-parameter and n is the total number of S-parameters (the dimensionality of the vector). Usually there are only absolute values of the measured S-parameters at the input. Therefore, the difference between each measured and computed S-parameter $(S_{gn} - S_{cn})$ is set by the difference of the absolute values. In this usual case the fitness value is evaluated as:

$$f_p = \sqrt{(|S_{g1}| - |S_{c1}|)^2 + (|S_{g2}| - |S_{c2}|)^2 + \cdots + (|S_{gn}| - |S_{cn}|)^2} \qquad (5.2)$$

It would be possible to use the Root Mean Square (RMS) which is very similar. But in this particular case the division before computation of the square root is an expensive mathematical operation from the point of view of the processing time of a central processing unit (CPU) and, moreover, it is not beneficial in this case due to the constant value in the denominator.

5.4   Software Description and Usage

The developed software is capable of running in the following three modes:

1. Estimation of relative permittivity/permittivities of a single or of a multi-layered structure: this is the default behaviour of the software. Its processing is based on the following arguments: thickness per layer (in meters, space-separated) along with a file containing frequencies and corresponding S-parameters. S2P and CTI file formats are supported. Otherwise a provided text file has to contain the space-separated frequency and corresponding transmission coefficient parameter per line.

   Example of running the estimation of permittivity of a structure containing three layers with their thicknesses of 6, 4 and 6 mm and which has measured S-parameters stored in a file named *measured.s2p*:

   ```
   permittivity.exe 0.006 0.004 0.006 measured.s2p
   ```

2. Synthesis of S-parameters of a single or of a multi-layered structure: to run
   the software in this mode the input arguments must start with selection
   of this mode (`-g` or `--generate-s-parameters`) followed with the number
   of layers, the minimal frequency, the maximal frequency, the number of
   frequency points, thickness (in meters) and complex permittivity per layer
   and, finally, with a file name in which the synthesized S-parameters should
   be stored.

   Example of running the synthesis of S-parameters in a frequency range
   from 1 to 20 GHz using 201 frequency points of a two-layered structure
   with the thicknesses of 3 and 4 mm, 2.05 - j0.04 and 4.2 - j0.08 complex
   relative permittivity:

   ```
   permittivity.exe -g 2 1e9 2e10 201 0.003 2.05 0.04 0.004 4.2 \
   0.08 synthetic.log
   ```

3. Estimation of relative permittivity/permittivities of a single or of a multi-
   layered structure with addition of a noise of normal distribution and spec-
   ified standard deviation to the input S-parameters: to run the software
   in this mode the input arguments must start with selection of this mode
   (`-n` or `--add-noise`) followed with the value of desired relative standard
   deviation (percentage), thickness per layer (in meters) and finally with a
   file name containing the input S-parameters.

   The noise is applied on all the input S-parameters in the following way:

$$S'_g \ = \ S'_{in}R(\mu,\sigma) \qquad\qquad (5.3)$$

$$S''_g \ = \ S''_{in}R(\mu,\sigma) \qquad\qquad (5.4)$$

where S'_{in} and S''_{in} are the real and the imaginary parts of the complex input
S-parameter read from the input file, $R(\mu,\sigma)$ represents a pseudorandom
numbers generator of normal distribution with mean $\mu = 1.0$ and standard
deviation σ is deduced from the relative standard deviation set by the
parameter (as mentioned above and described below). S'_g and S''_g represents
the real and the imaginary parts of the given complex S-parameter used
in the further processing in the algorithm.

Relative standard deviation (RSD, also known as the coefficient of variation) is used in order to provide better readability and possibly easier understanding in the rest of this doctoral thesis. RSD is equal to standard deviation σ divided by mean μ [46]:

$$c_v = \frac{\sigma}{\mu} \tag{5.5}$$

With respect to the mean $\mu = 1.0$ the value of RSD is equal to the value of standard deviation σ in the case of application of noise to the input S-parameters in this doctoral thesis. Therefore, RSD may be expressed as a percentage. RSD is the parameter given by a user running the software. Example below describes its usage.

Example of running the estimation of permittivity of a structure containing three layers of thicknesses 6, 4 and 6 mm and with corresponding measured S-parameters stored in a file named *measured.s2p*, adding noise of a normal distribution and RSD of 5 % to the input S-parameters (therefore, the standard deviation is equal to 0.05):

```
permittivity.exe -n 5 0.006 0.004 0.006 measured.s2p
```

Details about possible obligatory and optional command line arguments of the software are shown when running the program without any parameters (as well as with wrong parameters).

5.5 Simplifications

Introduced approach is quite complicated with respect to the nature of this inverse problem. The problem of estimation of permittivities of multi-layered structures from S-parameters seems not to be explicit. Therefore, the problem is not closed to just one solution, it is ambiguous, not deterministic and more solutions may be produced. Then there is also a space for some expert system limitations (like some reasonable expectable boundaries of relative permittivities). The more unknown variables to be estimated (more layers, more dimensional space has to be searched) the more complicated and longer pro-

cessing along with a risk of possibly higher number of possible solutions. This problem becomes hard to solve for more than one unknown layer with respect to the real and the imaginary part of the complex permittivity. Therefore, in the simplified case when the thickness of each layer is known there are two unknowns per layer. For two layers there are four unknowns, six unknowns for three layers. That is why this is the right place for utilization of EAs.

Considering such a multi-objective problem the situation could be intentionally simplified in neglecting the fact that the permittivity could (and very probably does) depend on frequency. In this work the real part of the complex permittivity is wilfully considered as a constant (in a narrow frequency range). This is highly important to mention at this place. This shortage can be removed in the future after incorporation of this specific part into the whole system.

6   EXPERIMENTS

The whole system presented in this doctoral thesis has been implemented using C++, a programming language, including the direct mathematical model computing the coefficients of transmission and the EA (PSO). The final software instrument has to be tested to verify its correctness. Therefore, several experiments have to be performed. There are three main kinds of experiments:

1. The software must be tested using synthetic data of single and multi-layered structures generated by the implemented direct mathematical model to verify the capability of the backward reconstruction using the selected EA.

2. The software must be tested using noisy synthetic data of single layers as well as on data of multi-layered structures to test the reasonable robustness of the backward reconstruction.

3. The software must be tested also using S-parameters obtained by direct measurements of single layers as well as of multi-layered structures of several materials to verify the inner direct mathematical model computing

S-parameters and the whole system in general. This kind of tests represents the most difficult cases.

6.1 Materials Under Test

Several experiments have been done with aluminium oxide, FR-4, plexiglass, polytetrafluoroethylene and RO4003. These materials have been already successfully defined and standardized in the past. These dielectrics have clear material properties and ease of access. Therefore, they are suitable for experiments in this work. These materials are described below in more detail.

The combinations of materials in multi-layered structures in the following experiments does not have a practical meaning (or it was not intended at least). They are just combined for testing purposes without any subsidiary intentions.

6.1.1 Aluminium Oxide

Aluminium oxide is a standard dielectric material. It is a white odourless crystalline powder. The mineral corundum is used to produce precious gems, such as ruby and sapphire. Activated aluminas are used extensively as adsorbents because of their affinity for water and other polar molecules; and as catalysts because of their large surface area and appropriate pore structure. As adsorbents, they are used for drying gases and liquids; and also in adsorption chromatography [48].

Few points about the material under test:

- Chemical formula: Al_2O_3.

- Short name: Alumina or Corundum.

- Relative permittivity at 17 GHz: 9.424 (depends on the purity of the selected material under test, 99.6 % Alumina in this case); loss tangent: 0.00031 [51].

- A photo of this sample is presented in Fig. 6.1 and its microstructure also in Fig. 6.2.

- Shape of the material under test: block.

- Dimensions of the material under test: 50 mm x 50 mm x 10 mm.

6.1.2   FR-4

FR-4 is one of the most widely used dielectric substrates in the fabrication of printed circuits for fast digital devices. This material exhibits substantial losses and the loss tangent is practically constant over a wide band of frequencies. It is used both for classical boards and for multi-layered boards. This composite material consists of glass fibres embedded in an epoxy resin [17].

Few points about the material under test:

- Complex relative permittivity at 1 GHz: $4.2 - j0.084$; loss tangent: 0.02 [17].

- Photos of this material are presented in Fig. 6.3 and also in Fig. 6.4.

- Shape of the material under test: sheet.

- Thickness of the material under test: 1.57 mm in the waveguide experiment and 1.53 mm in the free space experiments.

6.1.3   Plexiglass

Plexiglass, poly-methyl-methacrylate (PMMA), is an acrylic transparent thermoplastic light material [63].

Few points about the material under test:

- Complex relative permittivity at 10 GHz: $2.5 - j0.02$; loss tangent: 0.005 [63].
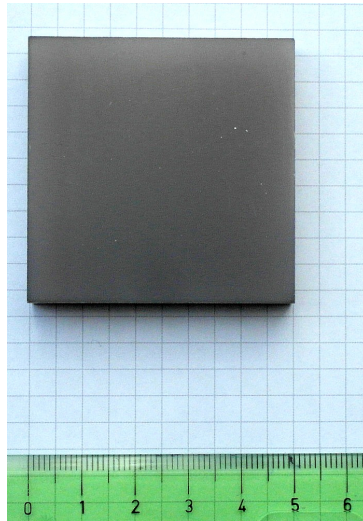
Fig. 6.1 A photo of aluminium
oxide used in the experiments
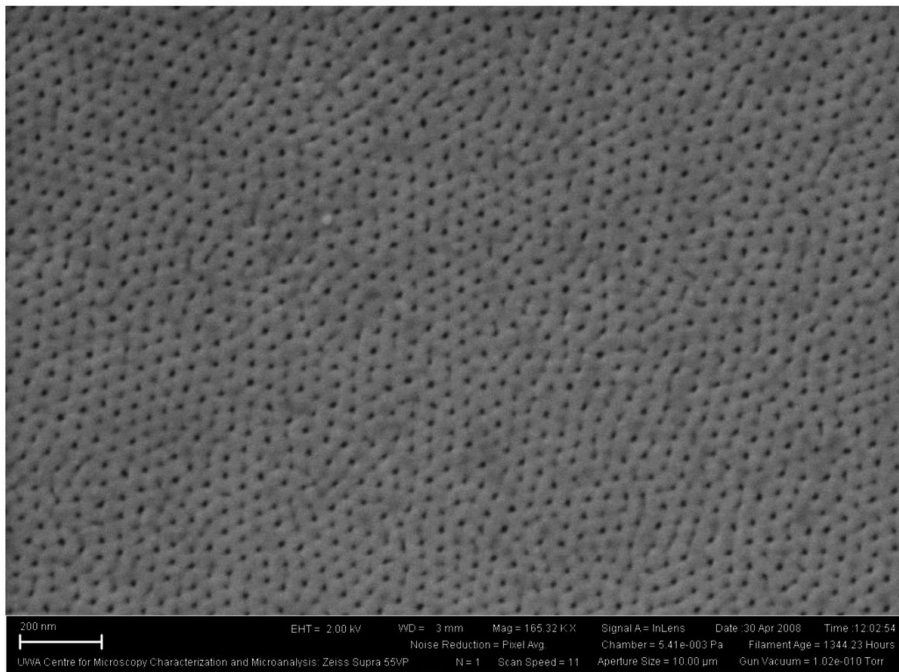
Fig. 6.2 A surface of aluminium oxide in a detail from an electron
microscope [50]
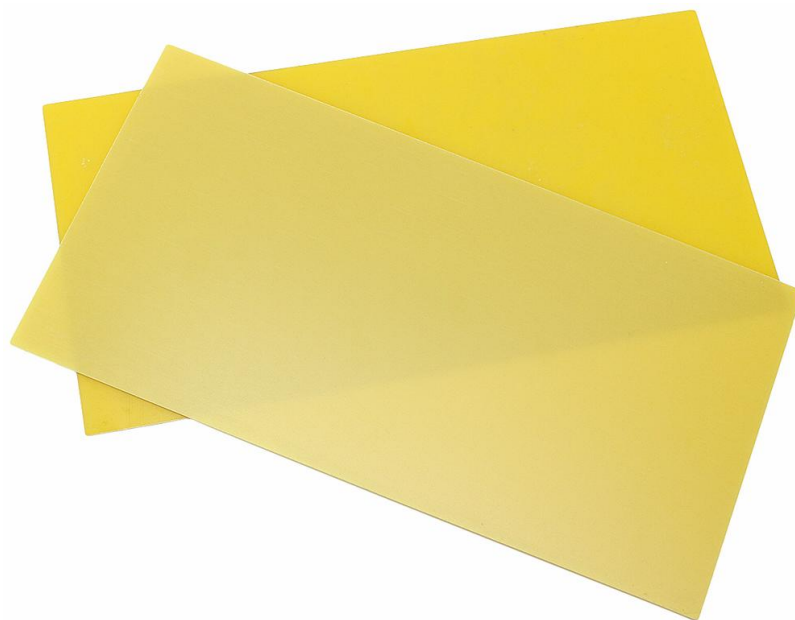
Fig. 6.3 View of two sheets of FR-4 [3]
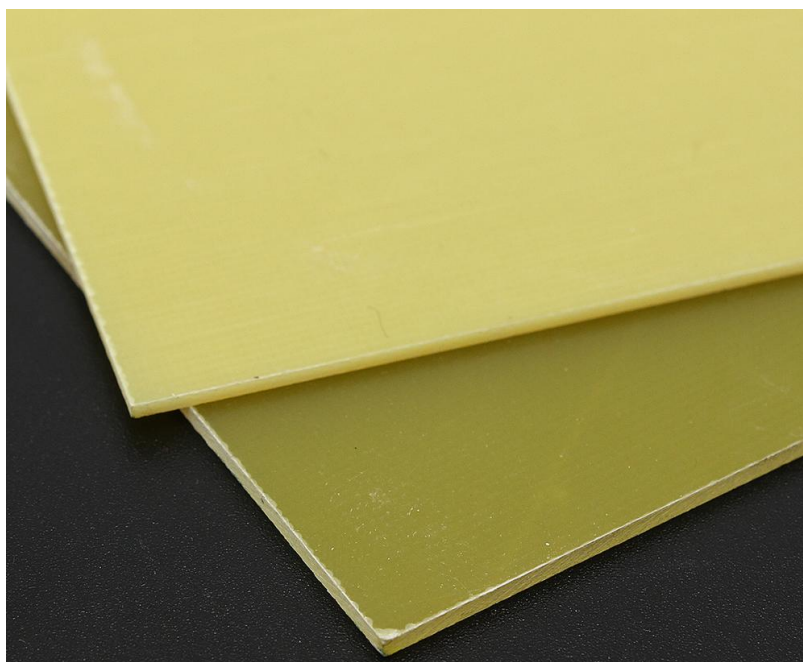
Fig. 6.4 View of two sheets of FR-4 in more detail [3]
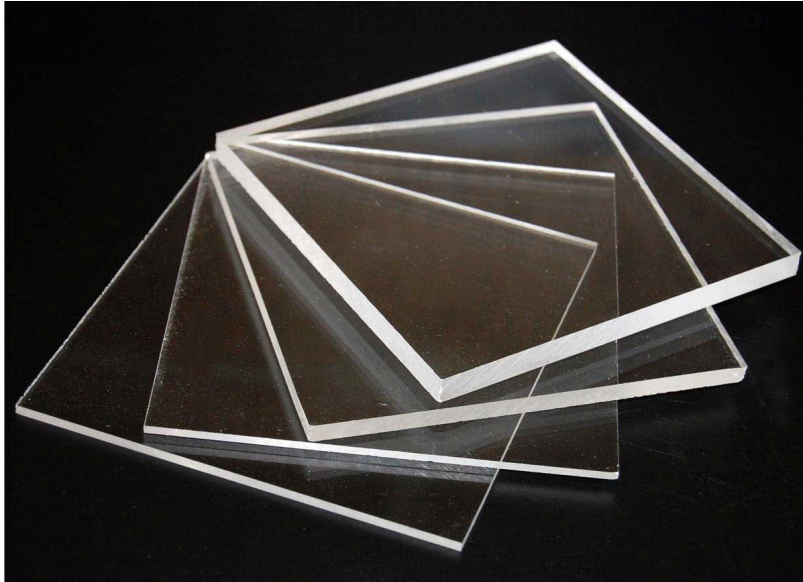
Fig. 6.5 Several transparent sheets of plexiglass of various
thicknesses [59]

- A photo of this sample is presented in Fig. 6.5.

- Shape of the material under test: sheet.

- Thickness of the material under test: 3.66 mm.

6.1.4 Polytetrafluoroethylene

Polytetrafluoroethylene (PTFE) is semi-crystalline in nature with complex struc-
tures even at ambient conditions. Due to the C-F bonds, it exhibits special prop-
erties surpassing those of most polymers such as very high melting temperature
(600 K) when compared to other crystalline polymers, good chemical resistance,
a low friction coefficient and good dielectric properties. In particular, its dielec-
tric properties have always attracted much interest for electronic applications
such as a high voltage equipment, cable insulators and printed circuit boards
[61].

Few points about the material under test:

- Brand name: "Teflon", developed by Chemours in 1938, commonly known as PTFE.

- Complex relative permittivity at 3 GHz: $2.05 \pm 0.05 - j0.04$; loss tangent: 0.00028 [61].

- A photo of this sample is presented in Fig. 6.6 and its microstructure also in Fig. 6.7.

- Shape of the material under test: cylinder.

- Dimensions of the material under test: 50 mm diameter, two variants of the thickness: 2.1 mm and 3.0 mm.

6.1.5   RO4003

RO4003 is a substrate for microwave circuits with low dielectric tolerance and loss, suitable for multilayer and mixed dielectric constructions. The temperature coefficient of dielectric constant is among the lowest of any circuit board material, and the dielectric constant is stable over a broad frequency range [54].

Few points about the material under test:

- Relative permittivity at 10 GHz: 3.38 ± 0.05; loss tangent: 0.0027 [54].

- A photo of this sample is presented in Fig. 6.8.

- Shape of the material under test: sheet.

- Thickness of the material under test: 1.52 mm.

6.2   Setup of the Evolutionary Algorithm

The Particle Swarm Optimization has been experimentally set to use 60 individuals in a swarm. Number higher than 100 usually makes the process of reconstruction ineffectively longer, without achieving a better precision [13].
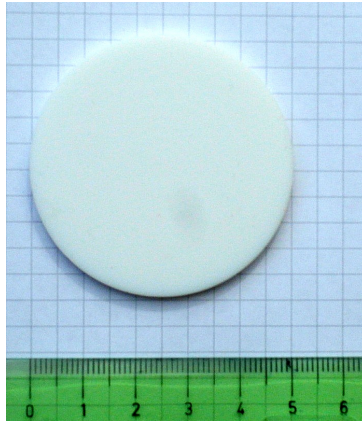
Fig. 6.6 A photo of
polytetrafluoroethylene used in
the experiments
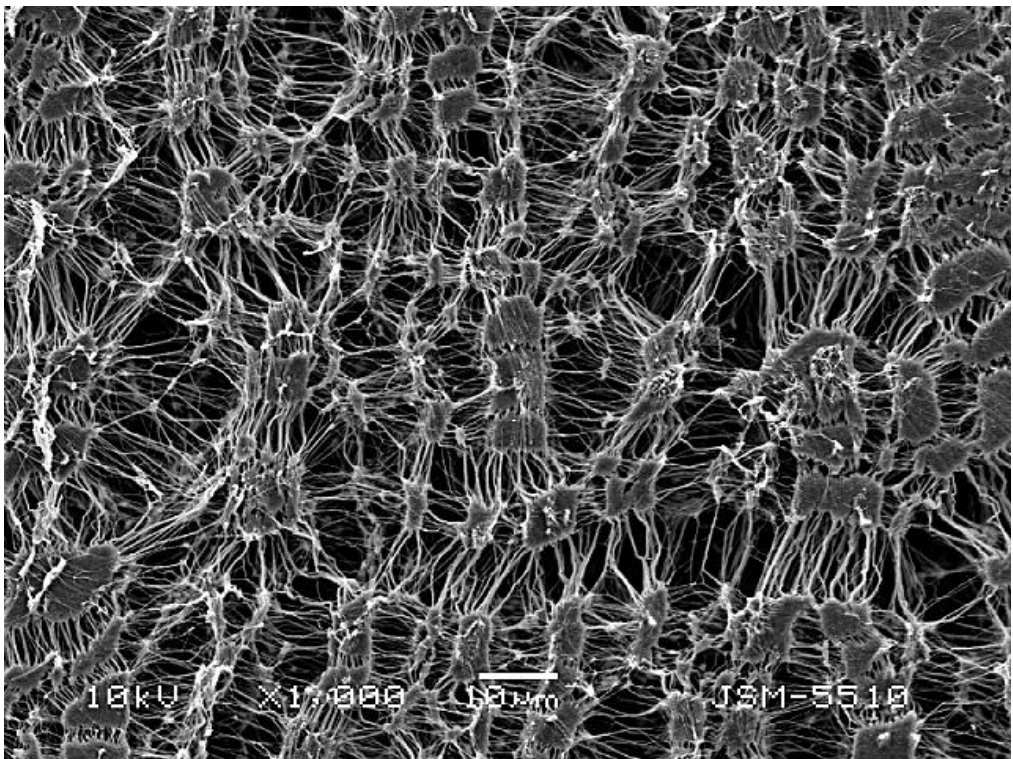
Fig. 6.7 Pure bi-axial expanded polytetrafluoroethylene with self adhesive strip
in a detail from an electron microscope [4]
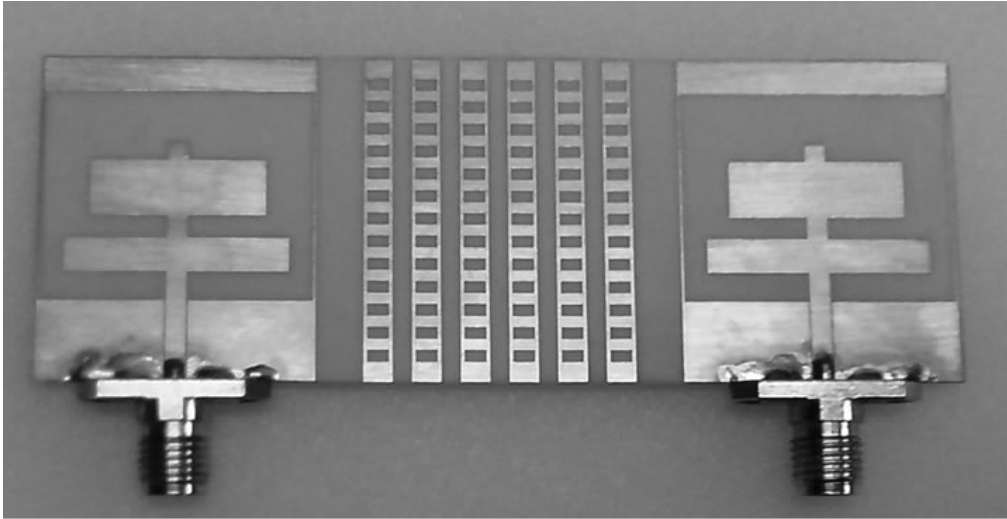
Fig. 6.8 An antenna etched on Rogers RO4003 substrate [14]

The EA is set up to stop if the fitness value (the square root of a sum of differences of computed and given S-parameters powered by two) is less than 10^{-7} or if the count of these evaluations is higher than 20 000 multiplied by the number of dimensions of solved problem (two dimensions for a single layer, four dimensions for a double layer etc.).

The lower and upper bound of a permittivity has been set up to the following intervals:

- [1.0, 15.0] for the real part of the complex permittivity, and

- [0.0, 1.0] for the imaginary part of the complex permittivity.

The upper bound has been set to the value of 15.0 which should represent a sufficient value for usually used solid dielectric materials (and with respect to the selection of materials under test in this work).

6.3   Test Computer

Subsequent experiments with the developed software have been run on a computer manufactured in 2016. It is Dell Latitude E5570 with processor Intel®️ Core™️ i7-6820HQ 4x 2.7 GHz, 16 GB RAM, operating system: Microsoft Windows 10 Professional 64-bit.

The software is executable also in Linux operating systems. The processing times in Linux are similar to the processing times in Microsoft's Windows operating system. However, they are not presented in this doctoral thesis.

6.4   Experiment #1: Waveguide Measurement of a Multi-Layered Structure

The first experiment was based on a cooperation with a foreign university. The author of this thesis was working one month with prof. Shestopalov in Karlstad University (Sweden) as a freemover (an exchange programme for scientists and young researchers). The title of the project was *"Parameter Optimization of Filters Employing Multi-Sectional Diaphragms in Waveguides of Rectangular Cross Section"*. Although the effort was aimed at waveguides some general principles remain and can be used also in free space measurements. The mathematical model generating S-parameters from known sections of materials placed in a waveguide has been created. Afterwards, an inverse estimation of the parameters of an unknown material in the waveguide was possible (using a numerical approach because of the non-explicit problem) [P.6].

The waveguide experiment took place in the Czech Republic, few months after the return from the internship in Sweden. A setup on which the mathematical background could be confirmed or rejected has been prepared. The material under test was not homogeneous but consisted of many sections what raised the complexity of the situation.

The details about the experiment were the following:

- Waveguide: R100 (22.86 mm × 10.16 mm).
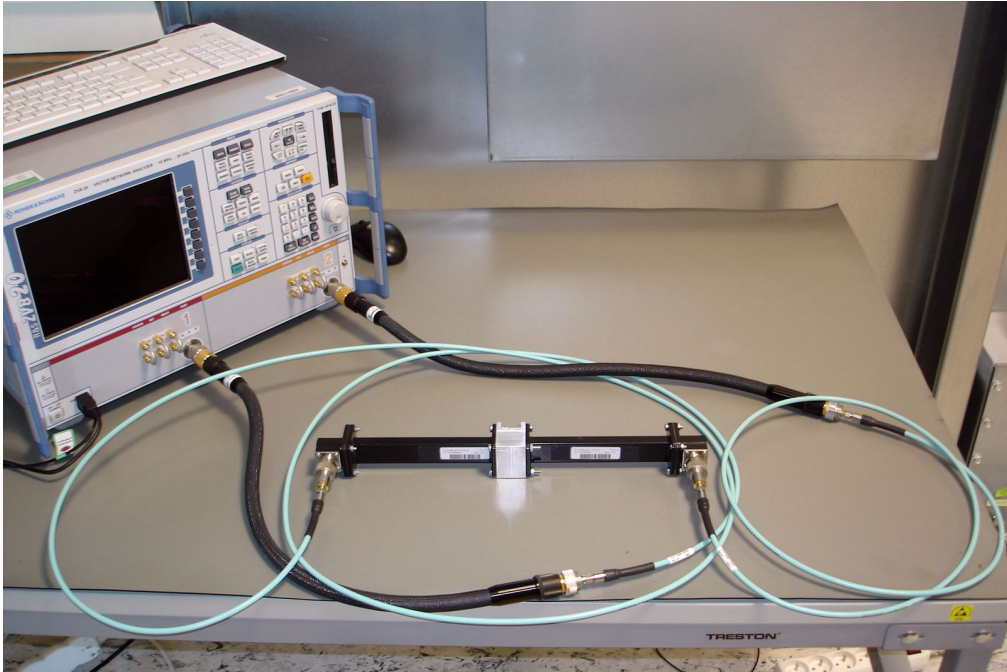
Fig. 6.9 Waveguide experiment: a photo of the measurement, waveguide is in the middle, VNA is on the left

- Frequency band: 8 GHz – 12 GHz.

- VNA: Rohde & Schwarz ZVB 20.

- Filter consisted of the following combination of eight sections (the incident wave was perpendicular to layers in this order): RO4003 | FR-4 | plexiglass | FR-4 | plexiglass | FR-4 | plexiglass | RO4003.

Fig. 6.9 illustrates the measurement line. The waveguide R100 included a block containing the sandwich of sections of materials arranged in the order mentioned above. The waveguide was connected to a calibrated vector network analyser Rohde & Schwarz ZVB 20.

Subsequently, Fig. 6.11 presents a photo of the sandwich structure where the changing layers of RO4003 on the sides, three thin FR-4 and three thicker plexiglass sections can be seen.

Fig. 6.10 shows a special profile which is used as a container for the sandwich to be measured.

To briefly present the final part of the mathematical background the explicit expression of the transmission coefficient for a one-sectional diaphragm ($n = 1$) is expressed in Eq. 6.1:

$$F = \frac{Ae^{i\gamma_0 l_1}}{g(z)} \tag{6.1}$$

where A is the amplitude of incident wave and $g(z)$ with z are described in Eq. 6.2 and Eq. 6.3:

$$g(z) = \cos z + i\left(\frac{z}{2\gamma_0 l_1} + \frac{\gamma_0 l_1}{2z}\right)\sin z, \tag{6.2}$$

$$z = l_1\gamma_1, \tag{6.3}$$

where l_1 is the thickness of the section, γ is computed in the way presented in Eq. 6.4:

$$\gamma_1 = \sqrt{k_1^2 - \left(\frac{\pi}{a}\right)^2}, \tag{6.4}$$

$$k_0 = \sqrt{\omega^2\epsilon_0\mu_0}, \quad k_1 = \sqrt{\omega^2\epsilon_0\epsilon_{r1}\mu_0}, \tag{6.5}$$

where k_1 is the wavenumber of the dielectric medium filling the section, a is the width of the section, $\omega = 2\pi f$ is the circular frequency, f is the field frequency, ϵ_0 is the permittivity of vacuum, ϵ_{r1} is the relative permittivity of a material of the section and μ_0 is the permeability of vacuum.

Fig. 6.12 just illustrates the measured data: the reflection coefficients S_{11} and S_{22} along with the transmission coefficients S_{21}.

Fig. 6.13 depicts the comparison between computed data and data obtained by direct measurement (transmission coefficients, S-parameter S_{21}). To quantify the difference of the two sets of data the Root Mean Square (RMS) has been used. RMS of the differences of absolute values of particular computed and measured S-parameters is equal to 0.0247. This difference is rather low, what confirms correctness of the mathematical model developed in Sweden (several
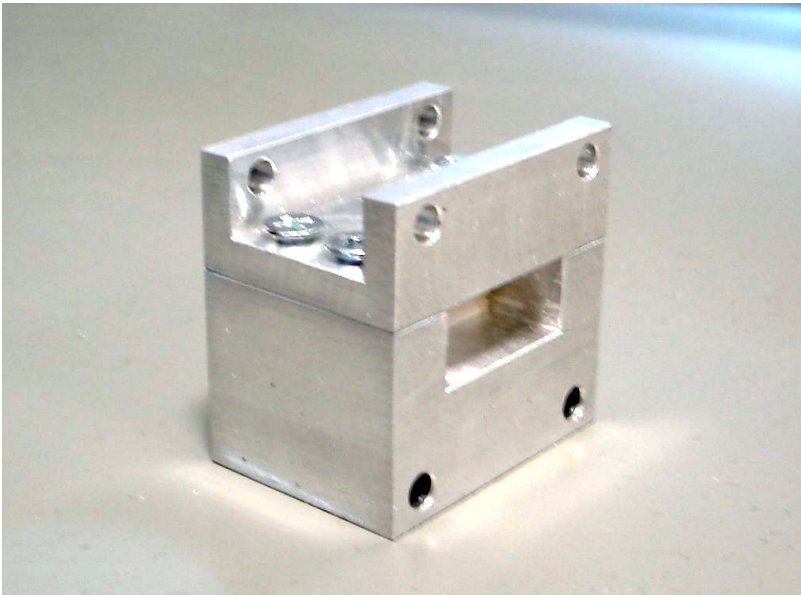
Fig. 6.10 The waveguide experiment: special profile for the
multi-layered structure of materials under test

Fig. 6.11 The waveguide experiment: a view of the
multi-layered structure of materials under test

other experiments should be preformed for verification). On such a complex problem, filter containing eight sections, the result seems to be very promising and further research could build other constructs on this relatively solid bases.

This experiment finally confirmed hypotheses on which the background mathematical propagation model stays.

6.5 Experiment #2: Synthetic Data of a Single Layer

This is the simplest experiment based on synthetic data computed by implemented free-space oriented direct model. This experiment tests the behaviour of the implementation of the EA. The developed software instrument should be capable of backward reconstruction of the complex permittivity of an imaginary material.

The imaginary material under test was polytetrafluoroethylene. S-parameters have been synthesized using complex relative permittivity $2.050 - j0.040$ (as typical for PTFE, described in subsection 6.1), thickness 3.0 mm, 201 frequency points from 1.0 GHz to 20.0 GHz).

The final estimated permittivity was exactly the same as the original permittivity set in the generation of the synthetic data, $2.050 - j0.040$ (in all of the 10 runs of the software). The average processing time was 1 303 ms (details about the computer which run this software are presented in the subsection 6.3).

The implementation of the EA seems to be verified with respect to the results of the single layer experiment.

6.6 Experiment #3: Synthetic Data of a Multi-Layered Structure

This experiment tests the backward reconstruction again. The focus in this test is set to a multi-layered structure.

The imaginary materials under test were aluminum oxide and polytetrafluoroethylene of thicknesses 10 and 3 mm. S-parameters have been synthesized
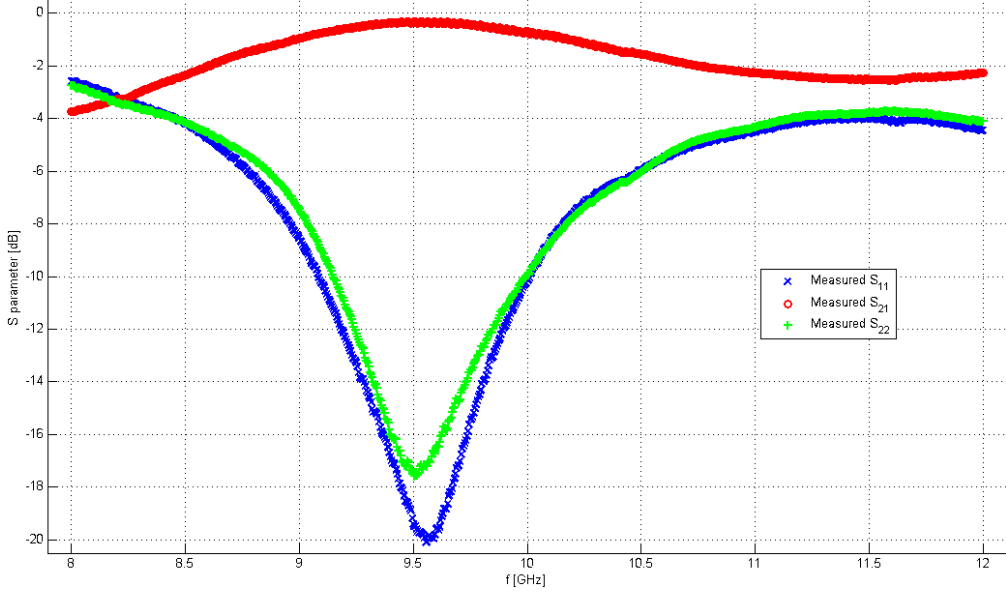
Fig. 6.12 The waveguide experiment: measured reflection S_{11}, S_{22} and transmission S_{21} coefficients
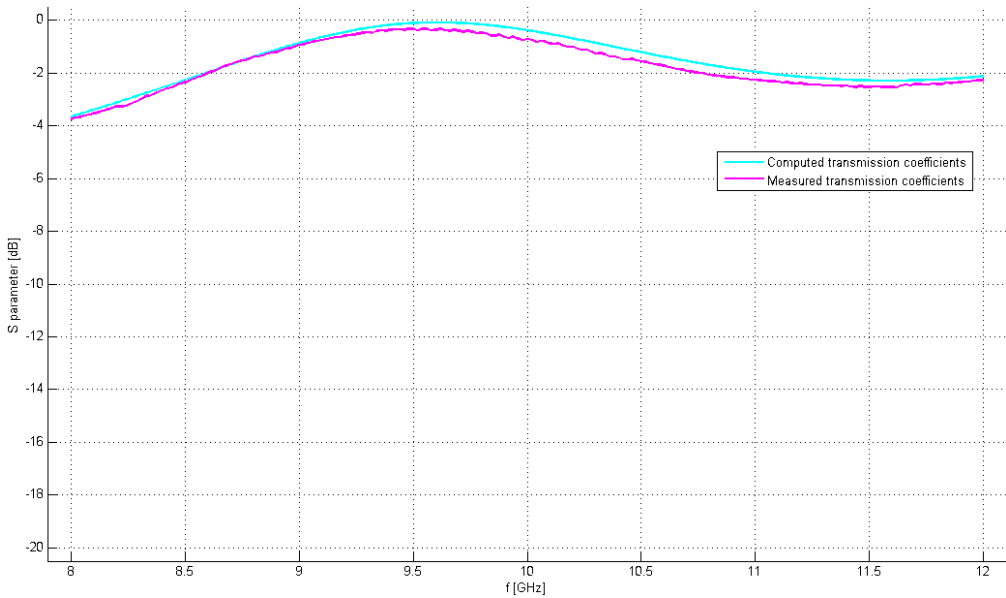
Fig. 6.13 The waveguide experiment: comparison of computed and measured transmission coefficients S_{21}

Tab. 6.1 Results of experiment #4 (using synthetic data of a single layer of PTFE with noise of 5% RSD)

Iteration	Estimated ϵ_r	Fitness (the best)	Processing time [ms]
1	$1.833 - j0.000$	0.621	1 046
2	$2.337 - j0.121$	0.598	1 285
3	$2.143 - j0.064$	0.656	1 290
4	$2.372 - j0.147$	0.642	1 316
5	$2.200 - j0.058$	0.603	1 286
6	$2.104 - j0.054$	0.586	1 293
7	$1.939 - j0.000$	0.579	1 260
8	$1.941 - j0.000$	0.602	1 022
9	$1.994 - j0.019$	0.525	1 284
10	$1.873 - j0.000$	0.584	1 004
Average	$2.0737 - j0.0463$	0.5996	1 208.6

using complex relative permittivities $9.424 - j0.0$ and $2.050 - j0.040$ (as typical for these materials, described in subsection 6.1), 201 frequency points from 1.0 GHz to 20.0 GHz).

The final estimated permittivities were exactly the same as the original permittivities set in the process of generation of the synthetic data, $9.424 - j0.0$ and $2.050 - j0.040$ (in all of the 10 runs of the software). The average processing time was 6 545 ms.

The implementation of EA seems to be verified with respect to the results of the 2-layered structure under test.

6.7 Experiment #4: Noisy Synthetic Data of a Single Layer

This is a continuation of the experiment #2. The imaginary material is the same, PTFE, with the same thickness and frequency points. The novelty of this experiment is in the application of some noise on the synthetic data of the single layer (normal distribution, RSD 5 %). This experiment tests the robustness of the backward reconstruction.

The average result was $2.0737 - j0.0463$ (the run of the software was repeated 10 times to get this average value, see Tab. 6.1). This final value is very close to the original complex relative permittivity of $2.050 - j0.040$. The difference between the real parts is only 0.0237 and 0.0063 in the imaginary parts of the expected and estimated complex relative permittivity. This represents 1.2% deviation (regarding the absolute values of the expected and the average estimated permittivity). The average processing time was $1\,208.6$ ms.

6.8 Experiment #5: Noisy Synthetic Data of a Multi-Layered Structure

This experiment represents another specific scenario which is more difficult for the software than in the previous experiment. In this case the robustness of the implemented backward reconstruction is tested on multiple layers including some additional noise of the normal distribution. A 2-layered and a 3-layered structures have been tested.

2-layered structure: The synthetic S-parameters of two layers of imaginary materials are used in this experiment. The structure consists of aluminum oxide and polytetrafluoroethylene. The thicknesses of the sections are 10.0 mm and 3.0 mm. S-parameters are synthesized at 201 frequency points, from 1.0 GHz to 20.0 GHz. Moreover, some noise has been added to the generated S-parameters also in this test (normal distribution, RSD 5 %).

The average estimated complex relative permittivity of the first and the second layer is:

1. $\epsilon_{r1}^* = 9.4319 - j0.0066$, and

2. $\epsilon_{r2}^* = 2.0519 - j0.0327$.

These are the average values from 10 runs of the software, see Tab. 6.2. The relative deviations in this experiment are equal to 0.1 % for both layers (regarding

Tab. 6.2 Results of experiment #5 (using synthetic data of a 2-layered structure of aluminum oxide & PTFE including normally distributed noise of 5% RSD)

Iteration	Estimated ϵ_{r1}	Estimated ϵ_{r2}	Fitness (the best)	Processing time [ms]
1	$9.448 - j0.000$	$2.030 - j0.030$	0.308	6 422
2	$9.457 - j0.012$	$2.048 - j0.030$	0.352	6 626
3	$9.429 - j0.018$	$2.077 - j0.035$	0.359	6 414
4	$9.429 - j0.010$	$2.074 - j0.035$	0.339	6 778
5	$9.395 - j0.000$	$2.040 - j0.050$	0.327	5 918
6	$9.469 - j0.017$	$2.083 - j0.022$	0.300	6 783
7	$9.385 - j0.000$	$2.057 - j0.058$	0.353	6 200
8	$9.448 - j0.000$	$2.024 - j0.029$	0.334	6 366
9	$9.432 - j0.010$	$2.056 - j0.010$	0.295	6 528
10	$9.429 - j0.000$	$2.031 - j0.030$	0.325	6 068
Average	$9.4319 - j0.0066$	$2.0519 - j0.0327$	0.3292	6 410.3

the absolute values of the expected and the average estimated permittivities of the layers).

3-layered structure: The synthetic S-parameters of three layers of imaginary materials are used in this experiment. The structure consists of polytetrafluoroethylene, air and polytetrafluoroethylene again (some kind of a sandwich structure). The thicknesses of the sections are 3.0 mm, 10.0 mm and 3.0 mm. S-parameters are synthesized at 201 frequency points, from 1.0 GHz to 20.0 GHz. Moreover, some noise has been added to the generated S-parameters also in this test (normal distribution, RSD 5 %).

The system responded well. The average estimated complex relative permittivity of the first, the second and the third layer is:

1. $\epsilon_{r1}^* = 2.0686 - j0.0395$,

2. $\epsilon_{r2}^* = 1.0031 - j0.0018$, and

3. $\epsilon_{r3}^* = 2.0231 - j0.0384$.

Tab. 6.3 Results of experiment #5 (using synthetic data of a 3-layered
structure consisting of PTFE & air & PTFE including normally distributed
noise of 5% RSD)

Iteration	Estimated ϵ_{r1}	Estimated ϵ_{r2}	Estimated ϵ_{r3}	Fitness (the best)	Processing time [ms]
1	$2.072 - j0.043$	$1.002 - j0.000$	$2.020 - j0.045$	0.544	14 536
2	$2.029 - j0.045$	$1.000 - j0.005$	$2.018 - j0.015$	0.524	15 289
3	$2.113 - j0.023$	$1.015 - j0.000$	$2.028 - j0.042$	0.542	14 781
4	$2.082 - j0.049$	$1.011 - j0.001$	$1.979 - j0.054$	0.510	15 539
5	$2.062 - j0.033$	$1.001 - j0.001$	$2.044 - j0.041$	0.497	15 855
6	$2.059 - j0.051$	$1.000 - j0.000$	$2.012 - j0.058$	0.514	14 799
7	$2.097 - j0.039$	$1.000 - j0.006$	$1.976 - j0.017$	0.479	15 648
8	$2.057 - j0.041$	$1.000 - j0.006$	$2.021 - j0.033$	0.529	15 501
9	$2.019 - j0.036$	$1.000 - j0.000$	$2.091 - j0.045$	0.447	14 419
10	$2.097 - j0.034$	$1.003 - j0.000$	$2.042 - j0.034$	0.526	14 589
Average	$2.0686 - j0.0395$	$1.0031 - j0.0018$	$2.0231 - j0.0384$	0.5112	15 095.6

These are the average values from 10 runs of the software, see Tab. 6.3. The relative deviations in this experiment are equal to 0.9 %, 0.3 % and 1.3 % (regarding the absolute values of the expected and the average estimated permittivities of the layers). The average estimated permittivities are very close to the original (expected) complex relative permittivities. This confirms some robustness of the backward reconstruction system.

6.9 Experiment #6: Measured Data of Single Layers

This is the first experiment in which a direct measurement of S-parameters in free space occurs. Only single sections of materials have been tested in this experiment (firstly polytetrafluoroethylene of various thicknesses and secondly aluminium oxide).

The measurements presented in this experiment took place at the Department of Dielectrics at Institute of Physics of the Czech Academy of Sciences in Prague [16]. The spectral analysis was processed by infrared Fourier transform spectrometer BRUKER 113v. It operates in vacuum in the near, middle and far infrared spectral ranges. Its sample compartment could be purged with nitrogen or argon in order to reduce absorption bands of CO_2 and water vapour. Other technical details of the used spectroscope follows:

- spectral range: 10 000 to 10 cm^{-1},

- resolution: 0.03 cm^{-1},

- wavenumber accuracy: 0.01 cm^{-1} at 2 000 cm^{-1},

- sources: Globar 6 000–10 cm^{-1}, Hg Arc 700–10 cm^{-1}, Tungsten-Halogen 10 000–1 850 cm^{-1},

- detectors: DTGS with KBr window 7 000–400 cm^{-1}, DTGS with Polyethylene window 600–10 cm^{-1}, MCT 5 000–600 cm^{-1},

- interferometer: fully automatized Genzel interferometer,

- scan Velocity: 1.6–12.7 mm/sec opd, and

- sample compartment [cm]: 25.5 (w) x 27 (d) x 16 (h) purgeable.

Fig. 5.2 illustrates the experimental test bench with an emitting and a receiving antenna connected to a calibrated analyser with a sample under test placed in between.

This experiment is crucial from the point of view of testing the ability of the developed software to work with real data. EA with the capability of the backward reconstruction has been proven in the previous experiments. Data from direct measurements are used in this step to test the correctness of the direct mathematical model and consequently the whole system.

Polytetrafluoroethylene: This material has been measured on 51 frequency points from 839 GHz to 1 562 GHz. The average estimated complex permittivity was $2.671 - j0.0$ for the 2.1 mm thick sample and $4.8014 - j0.00008$ for the 3.0 mm thick sample, the average processing time was 270.5 ms, 272.6 ms respectively (average values from 10 runs of the software, see Tab. 6.4 and Tab. 6.5 for details). These average values are far from the expectations (see subsection 6.1 for details about materials under test and their properties). The relative deviation of the average estimated permittivity is equal to 30.3 % for the 2.1 mm thick sample and 134.2 % for the 3.0 mm thick sample (regarding the absolute values of the expected and the average estimated relative permittivity). Nevertheless, these deviations are pure statistical numbers (this approach is consistent in all the experiments in this doctoral thesis). Looking at the results of 3.0 mm thick sample of PTFE presented in Tab. 6.5 possible doubts about the final average value may appear. The real part of the estimated permittivity is equal to 3.018 in 8 from 10 cases. However, the real part jumped nearly to 12 in the remaining 2 cases what is very different nearly 4-times higher result then in the majority. Therefore, some kind of post-processing/heuristics which will eliminate these very different isolated values (high peaks or deep holes in an array of results) may take place. The author of this doctoral thesis propose to discuss and implement some kind of treatment in the further research. The average estimated complex

permittivity of the 3.0 mm thick sample of PTFE would be $3.018 - j0.000$ (47.2% relative deviation regarding the expected absolute value) if the unusual wrong peak estimations were neglected.

Additional note about the 3.0 mm thick sample of PTFE relates to the fitness values of the best particles in the PSO. There are two unusual isolated high peaks in the row of estimated permittivity (as presented in the previous paragraph, see Tab. 6.5). It is surprising that right these two very wrong results have the lowest fitness value what should mean that these results are more close to the true value than the others. This is in contrary to expectations.

Such wrong results and strange fitness values may relate to the thin layer which could be more difficult for processing. Moreover, wide frequency range has been used (723 GHz) what may be too much for considering the permittivity as a constant. Also some kind of an error in the measurement system could occur. Only one measurement has been performed (without any repetition). Therefore, revision and repetition of the measurement should take place. Also this may be one of the goals of the further work.

Aluminium oxide: This material has been measured on 805 frequency points from 376 GHz to 12 004 GHz what is a huge frequency range of overstepping of two orders from hundreds of GHz up to tens of THz. The average estimated complex relative permittivity was $9.808 - j0.019$, the average processing time was 4 147 ms (average values from 10 runs of the software, see Tab. 6.6 for details). This result is close to the expected permittivity, therefore, it may be considered as acceptable. The relative deviation of the average result is equal to 3.3 % (regarding the absolute values of the expected and the average estimated relative permittivity).

6.10   Experiment #7: Measured Data of a Multi-Layered Structure

Also this measurement took place at the Department of Dielectrics at Institute of Physics of the Czech Academy of Sciences in Prague with the same measurement

Tab. 6.4 Results of experiment #6 (using measured data of a single layer of PTFE, 2.1 mm)

Iteration	Estimated ϵ_r	Fitness (the best)	Processing time [ms]
1	$2.671 - j0.0$	0.418	274
2	$2.671 - j0.0$	0.418	268
3	$2.671 - j0.0$	0.418	268
4	$2.671 - j0.0$	0.418	274
5	$2.671 - j0.0$	0.418	272
6	$2.671 - j0.0$	0.418	271
7	$2.671 - j0.0$	0.418	269
8	$2.671 - j0.0$	0.418	273
9	$2.671 - j0.0$	0.418	268
10	$2.671 - j0.0$	0.418	268
Average	$2.671 - j0.0$	0.418	270.5

Tab. 6.5 Results of experiment #6 (using measured data of a single layer of PTFE, 3.0 mm)

Iteration	Estimated ϵ_r	Fitness (the best)	Processing time [ms]
1	$3.018 - j0.0000$	0.286	274
2	$11.907 - j0.0001$	0.065	254
3	$3.018 - j0.0000$	0.286	270
4	$3.018 - j0.0000$	0.286	272
5	$3.018 - j0.0000$	0.286	266
6	$3.018 - j0.0000$	0.286	268
7	$3.018 - j0.0000$	0.286	274
8	$3.018 - j0.0000$	0.286	300
9	$11.962 - j0.0007$	0.057	284
10	$3.018 - j0.0000$	0.418	264
Average	$4.8014 - j0.00008$	0.2542	272.6

Tab. 6.6 Results of experiment #6 (using measured data of a single layer of aluminium oxide)

Iteration	Estimated ϵ_r	Fitness (the best)	Processing time [ms]
1	$9.576 - j0.083$	0.145	4 302
2	$9.756 - j0.083$	0.137	4 121
3	$9.756 - j0.083$	0.137	4 139
4	$9.757 - j0.083$	0.137	4 146
5	$9.756 - j0.083$	0.137	4 238
6	$9.756 - j0.083$	0.137	4 116
7	$9.756 - j0.083$	0.137	4 066
8	$9.757 - j0.083$	0.137	4 052
9	$9.759 - j0.084$	0.140	4 146
10	$9.756 - j0.083$	0.137	4 144
Average	$9.7387 - j0.0834$	0.1381	4 147

line as in the previous experiment.

A two-layered structure of Aluminum oxide and 3mm PTFE has been measured on 21 frequency points from 448 GHz to 737 GHz. The average estimated complex relative permittivity of the first material from the structure (Aluminum oxide) was $9.8642 - j0.00004$ and $1.8725 - j0.46995$ of the second material, the average processing time was 1 160.4 ms (average values from 10 runs of the application, see Tab. 6.7 for details).

These results' relative deviation is equal to 4.7 % and 5.8 % for the first and for the second material respectively (regarding the absolute values of the expected and the average estimated relative permittivity). These results are acceptable. They confirm the capability of the developed system to work with data from direct measurements of multi-layered structures.

6.11 Experiment #8: Measured Data of a Single Layer

The last direct measurement took place at Centre of Polymer Systems of Tomas Bata University in Zlin. FR-4 has been selected as the material under study in this experiment.

Tab. 6.7 Results of experiment #7 (using measured data of a multi-layered
structure consisting of aluminium oxide & PTFE)

Iteration	Estimated ϵ_{r1}	Estimated ϵ_{r2}	Fitness (the best)	Processing time [ms]
1	$9.717 - j0.0000$	$1.359 - j0.1415$	0.096	1 138
2	$9.722 - j0.0000$	$1.634 - j0.2127$	0.121	1 157
3	$9.719 - j0.0000$	$1.088 - j0.4145$	0.071	1 145
4	$9.712 - j0.0003$	$1.002 - j0.1008$	0.124	1 164
5	$9.732 - j0.0000$	$1.124 - j0.9999$	0.086	1 188
6	$9.732 - j0.0000$	$1.300 - j0.9281$	0.091	1 125
7	$11.13 - j0.0000$	$7.374 - j0.0001$	0.339	1 156
8	$9.720 - j0.0000$	$1.130 - j0.4209$	0.072	1 180
9	$9.732 - j0.0002$	$1.533 - j0.7480$	0.117	1 160
10	$9.727 - j0.0000$	$1.180 - j0.7328$	0.081	1 191
Average	$9.8642 - j0.00004$	$1.8725 - j0.46995$	0.1198	1 160.4

The measurement was based on utilization of Agilent Technologies N5230A PNA-L which was calibrated using mechanical standards (open, short, load and thru), 2-port (calibration kit 85052D). Technical details of the used network analyser follows [2]:

- working frequency from 300 kHz to 13.5 GHz, from 10 MHz to 50 GHz,

- 108 dB of dynamic range and <0.006 dB trace noise,

- <9 μsec/point measurement speed, 32 channels, 16 001 points, and

- TRL/LRM calibration, on-wafer, in-fixture, and waveguide measurements.

Fig. 6.14 shows the whole measurement line (the calibrated analyser connected to the transmitting and receiving antennas) while Fig. 6.15 presents the holder of samples with the antennas and finally Fig. 6.16 depicts the calibration standards in detail.

This material has been measured on 51 frequency points from 1.0 to 20.0 GHz. The average estimated complex relative permittivity was $4.506 - j0.0$. The
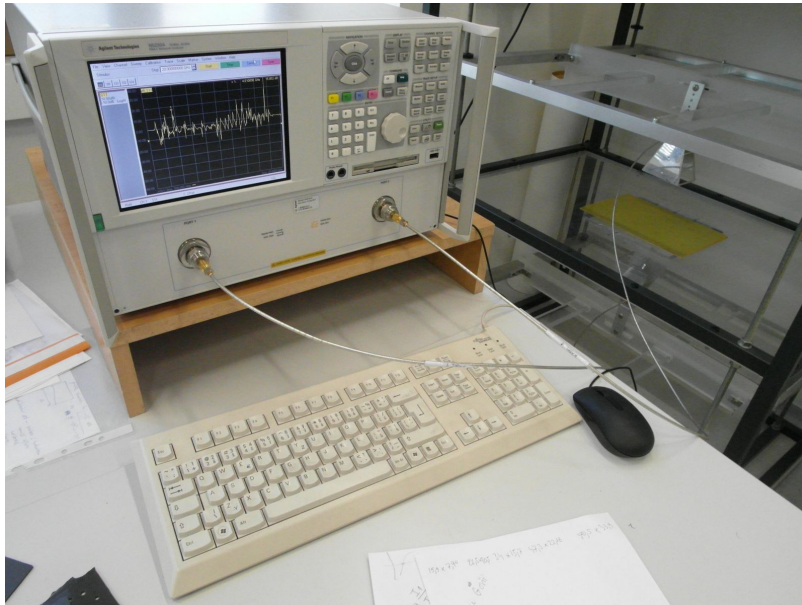
Fig. 6.14 Measurement line employing Agilent Technologies
N5230A PNA-L
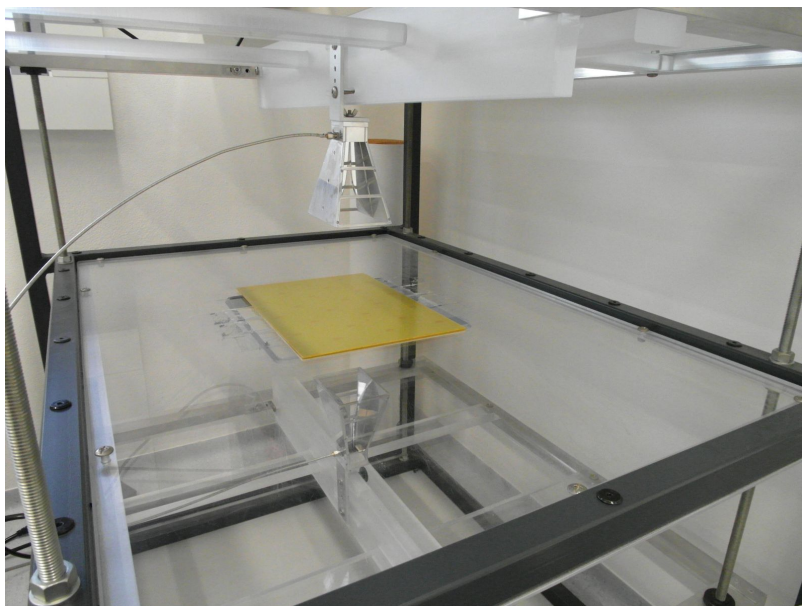
Fig. 6.15 Transmitting and receiving antennas with material
under test in between (FR-4)

Fig. 6.16 Calibration kit 85052D (open, short and load)

Tab. 6.8 Results of experiment #8 (using measured data of a
single layer of FR-4)

Iteration	Estimated ϵ_r	Fitness (the best)	Processing time [ms]
1	$4.506 - j0.0$	0.795	298
2	$4.506 - j0.0$	0.795	300
3	$4.506 - j0.0$	0.795	302
4	$4.506 - j0.0$	0.795	330
5	$4.506 - j0.0$	0.795	298
6	$4.506 - j0.0$	0.795	299
7	$4.506 - j0.0$	0.795	304
8	$4.506 - j0.0$	0.795	302
9	$4.506 - j0.0$	0.795	316
10	$4.506 - j0.0$	0.795	319
Average	$4.506 - j0.0$	0.795	306.8

average processing time was 307 ms (average values from 10 runs of the software, see Tab. 6.8 for details). The expected value was $4.2 - j0.084$. The relative deviation of the average result is equal to 7.3 % (regarding the absolute values of the expected and the average estimated relative permittivity).

6.12 Summary of the Experiments

Realization of experiments posed a more complicated task than expected. Acquisition of materials was rather easy part in comparison with negotiations with laboratories postponing the measurements. This is the main reason why the number of materials under test and the corresponding number of direct measurements is not very high. However, the number of experiments can be considered as sufficient for the need of confirmation of the individual pillars, approaches and implementations. All the results are promising except the experiment with polytetrafluoroethylene in the experiment # 6. A repetition of this experiment may reveal the source of the strong deviation.

6.12.1 Speed of the Software

The speed of the implemented system is noted in the tables and paragraphs in each free-space experiment above. The processing time mainly depends on the number of layers in the experiment, on the number of frequency points and also on the hardware on which the software is executed. Specification of the test computer which was running all the experiments is described in subsection 6.3.

The speed of the software is very promising considering the average processing time of the first simple experiment with synthetic data of a single layer and 201 frequency points that took only at about 1.3 second. In contrary, a much more difficult case represented by a 3-layered structure including some noise in the input data with 201 frequency points took at about 15.1 seconds in average.

7 UNCERTAINTY & SENSITIVITY ANALYSIS

Quantification of the uncertainty of any measurement is important since there is always a margin of doubt about the measurement. Definitions of few important terms follow to avoid confusion [7].

True value is the value that would be obtained by a perfect measurement.

Error is the difference between the measured value and the *true value* of the thing being measured.

Uncertainty is a quantification of the doubt about the measurement result.

The uncertainty of the estimation of complex relative permittivity is not analytically solvable due to the fact that the problem of permittivity reconstruction is not an explicit problem. ϵ_r cannot be computed directly using a mathematical formula (details in section 3). Therefore, the uncertainty is estimated statistically by a set of measurements & permittivity estimations (so called Type A evaluation [7]).

The source of error in the estimation of permittivity is represented by a combination of the error in the measuring instrument (for instance: bias, changes due to ageing, wear, noise, wrong calibration), the deviations in the material under test (for instance: non-homogeneousness, impurities) and environment issues (for instance: higher or lower temperature or humidity). The combination of all these influences leads to a mass error of the input data (S-parameters) to the evolutionary processing. Therefore, an input error represented by a relative standard deviation figures in the analysis below. For details about RSD see subsection 5.4.

Standard deviation σ is a usual quantification of spread of the values of measurements. It can be mathematically expressed as [7]:

$$\sigma = \sqrt{\frac{\sum_{i=1}^{n}(X_i - \overline{X})^2}{n-1}} \tag{7.1}$$

where X_i represents i-th scalar of the measurement vector of data and n stands for the number of measurements.

Standard uncertainty u estimated from statistics of a set of measurements is computed using the standard deviation σ and the number of measurements n:

$$u = \frac{\sigma}{\sqrt{n}} \tag{7.2}$$

Standard uncertainty is a margin informing about the uncertainty of an average (not just about the spread of values) [7].

7.1 Pseudorandom Number Generator

The role of the pseudorandom number generator (PRNG) is important not only in the process of evolution in EAs but also in the experiments adding some noise to the input S-parameters. The noise must be generated with desired probability distribution.

One of the key characteristics in SI measurements is jitter. It represents variations in the data signal. Typically, these variations behave statistically in nature. Random jitter usually follows a normal distribution [8].

Classical statistical methods that use the sample mean and standard deviation, under the assumption that the data follow a Gaussian (normal) distribution, are often applied to measurement inter-comparisons [33].

Standard random numbers generator available in C++ (since C++11) has been used in the software of this doctoral thesis. The histogram of a test case with 10 000 generated numbers is depicted in Fig. 7.1. The setup of the pseudorandom number generator was the following:

- normal distribution,

- mean $\mu = 0.0$, and

- standard deviation $\sigma = 1.0$.
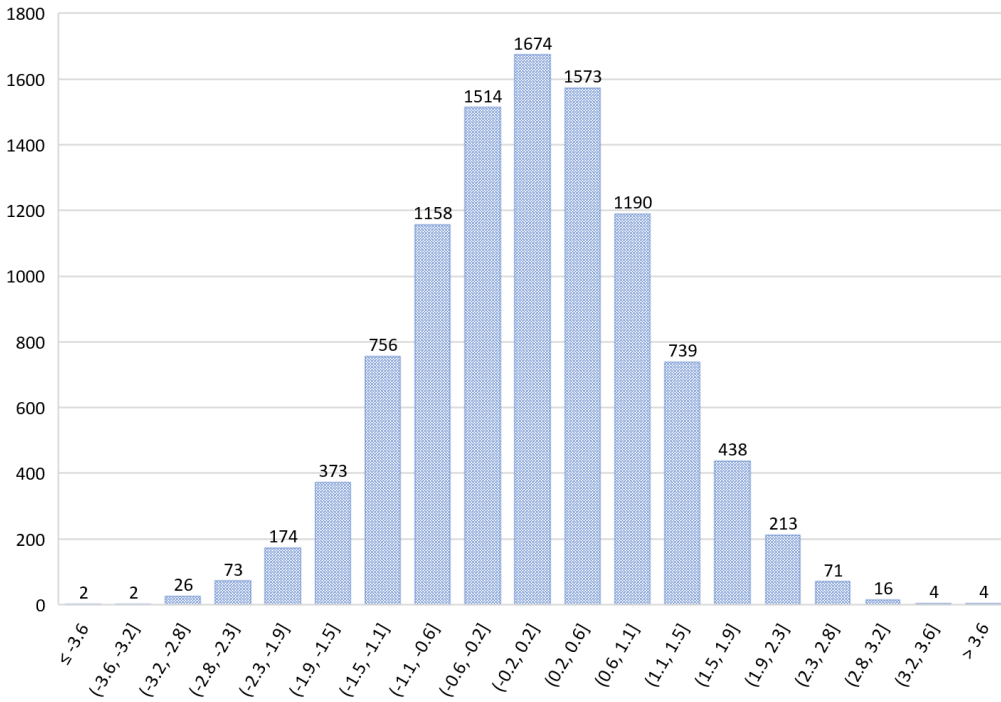
Fig. 7.1 Histogram of 10 000 numbers generated by selected PRNG (normal distribution, mean 0.0, standard deviation 1.0)

7.1.1   Pearson's Chi-Square Goodness of Fit Test

The histogram presented in Fig. 7.1 seems to correspond to the normal distribution. However, this hypothesis should be verified. For this purpose, the chi-square (χ^2) test has been applied on the pseudorandomly generated data. This test is used to confirm or reject a null hypothesis. In this case the null hypothesis relates to the kind of distribution of the input data, whether these data follow the normal distribution. The input data must be transformed into a histogram of a specified number of sections for the purpose of further processing.

χ^2 can be quantified in the following way [52]:

$$\chi^2 = \sum_{j=1}^{k} \frac{(O_j - E_j)^2}{E_j} \tag{7.3}$$

where k stands for the number of histogram sections, E_j is the expected count (also known as the *theoretical* value) of the j-th section of the histogram and O_j is the observed count (also known as the *empirical* value) of the j-th section of the histogram.

The empirical (observed) counts are created from the input data from a selected PRNG (as can be seen in Fig. 7.1). In spite of that the theoretical (expected) counts are precisely computed using mathematical formulas. In this case the expected histogram is prepared by the probability density function of the normal distribution [47]:

$$f(x, \mu, \sigma^2) = \frac{1}{\sigma\sqrt{2\pi}} e^{-\frac{(x-\mu)^2}{2\sigma^2}} \tag{7.4}$$

where $|x| < \infty$, $|\mu| < \infty$ and $\sigma > 0$. A normal distribution is called standard when $\mu = 0.0$ and $\sigma = 1.0$.

χ^2 follows the Pearson probability distribution with n degrees of freedom:

$$n = k - r - 1 \tag{7.5}$$

where r stands for the number of parameters of the probability density function. The χ^2 along with the number of degrees of freedom is then used to compute the probability using the Pearson probability distribution F_p:

$$p = F_p(\chi^2, n) \tag{7.6}$$

The probability p is then compared to the significance level α (commonly set to 0.05 [15]). If $p > 1 - \alpha$ then the tested hypothesis is rejected on the significance level α [52].

7.1.2 Testing the Probability Distribution of Selected PRNG

Working with observed data generated by selected PRNG (section 7.1), the null and the corresponding alternative hypotheses have been defined the following way:

- H_0: The observed data from the selected PRNG are normally distributed.

- H_A: The observed data from the selected PRNG are not normally distributed.

Configuration of the test:

- The PRNG has been set up to produce numbers following the standard normal distribution ($\mu = 0.0$, $\sigma = 1.0$).

- Histogram is portioned into $k = 20$ segments.

- The significance level in this test has been set to $\alpha = 0.05$ (common threshold [15]).

- The sum of the empirically counted numbers is equal to the sum of generated numbers assigned to the histogram, what is nearly 100 000 (it is exactly only 99 992, it is not rounded to thousands due to the nature of the normal distribution and the fact that the histogram is segmented into a specific number of segments).

Histograms of the expected data and a test set of observed data generated by the selected PRNG are presented in Tab. 7.1. Repeating the process of generation of a new test set of pseudorandom numbers gives little bit different results all the time but the results are usually similar to the following ones.

Results:

- $n = 17$,

- $\chi^2 = 24.961$, and

- $p = 0.929$.

Tab. 7.1 Histograms of the expected and observed
random data (generated by the selected PRNG) of
standard normal distribution

Interval	Expected count	Observed count
$[-3.60, -3.24)$	41	45
$[-3.24, -2.88)$	133	148
$[-2.88, -2.52)$	375	392
$[-2.52, -2.16)$	929	948
$[-2.16, -1.80)$	2 023	2 099
$[-1.80, -1.44)$	3 867	3 886
$[-1.44, -1.08)$	6 495	6 516
$[-1.08, -0.72)$	9 581	9 640
$[-0.72, -0.36)$	12 417	12 227
$[-0.36, 0.00)$	14 135	14 163
$[0.00, 0.36)$	14 135	13 953
$[0.36, 0.72)$	12 417	12 395
$[0.72, 1.08)$	9 581	9 564
$[1.08, 1.44)$	6 495	6 553
$[1.44, 1.80)$	3 867	3 834
$[1.80, 2.16)$	2 023	2 080
$[2.16, 2.52)$	929	988
$[2.52, 2.88)$	375	357
$[2.88, 3.24)$	133	151
$[3.24, 3.60)$	41	53

Conclusion: H_0 is accepted on the significance level alpha ($p \leq 1 - \alpha$, where $\alpha = 0.05$).

This test has been repeated and the hypothesis H_0 was accepted in 9 from 10 cases (10 test sets of pseudorandom numbers). Therefore, the numbers generated by the selected PRNG follow the normal distribution.

7.2 Experimental Setup

The input data (S-parameters) in these experiments must be strictly correct to evaluate proper total output uncertainty of the result and sensitivity analysis

on the controlled artificial input error. These input data have been synthesized in the frequency range from 1 to 20 GHz. This rather narrower range has been selected so as to consider constant real part of complex permittivities of the materials under test, moreover, without complications caused by resonances. The number of repetitions of all the tests in these analyses has been set to 100.

Various tests have been run. The list of varied aspects follows:

- the number of layers of materials under test: a single layer, 2-layered and 3-layered structures,

- the number of frequency points: 201 for the basic setup and 402 for the extended setup to partially express the influence of the granularity of the input data (hypothesis: the higher number of measurements the potentially easier way to get closer to the true values), and

- the RSD of the error of the input data: 0, 1, 2, 5, 10 and 20 %.

7.2.1   A Single Layer

Plexiglass material has been selected for the single layer experiment ($\epsilon_r = 2.5 - j0.02$, 3.66mm thickness, for further details of this material see subsection 6.1). The estimated complex relative permittivity with statistically defined standard uncertainty and analysis of sensitivity on error level of the input data using 201 frequency points is presented in Tab. 7.2. Tab. 7.3 contains results related to 402 frequency points of the input.

The mean values of the real and the imaginary parts of the complex relative permittivity including uncertainties are depicted in Fig. 7.2. As expected, the softer granularity of the input data helps achieve results closer to the true values.

7.2.2   A 2-Layered Structure

A 2-layered structure represents a more complicated situation (due to the four-dimensional optimization problem). The combination of 3.0mm thick PTFE

Tab. 7.2 Estimated complex relative permittivity with statistically defined standard uncertainty along with sensitivity analysis on RSD of the error of the input data, a single layer of plexiglass, expected $\epsilon_r = 2.5 - j0.02$, 201 frequency points

Noise RSD	$\overline{\epsilon_{r\ real}} \pm u_{real}$	$\overline{\epsilon_{r\ imag}} \pm u_{imag}$	$\overline{t}\ [ms]$
0 %	2.5 ± 0.0	$0.02 \pm 1.4 \exp(-18)$	1 371.4
1 %	2.4987 ± 0.0016	0.01988 ± 0.00032	1 358.2
2 %	2.4990 ± 0.0035	0.01988 ± 0.00067	1 349.0
5 %	2.4977 ± 0.0069	0.0222 ± 0.0016	1 300.4
10 %	2.516 ± 0.014	0.0308 ± 0.0026	1 326.8
20 %	2.550 ± 0.028	0.0520 ± 0.0049	1 395.8

Tab. 7.3 Estimated complex relative permittivity with statistically defined standard uncertainty along with sensitivity analysis on RSD of the error of the input data, a single layer of plexiglass, expected $\epsilon_r = 2.5 - j0.02$, 402 frequency points

Noise RSD	$\overline{\epsilon_{r\ real}} \pm u_{real}$	$\overline{\epsilon_{r\ imag}} \pm u_{imag}$	$\overline{t}\ [ms]$
0 %	2.5 ± 0.0	$0.02 \pm 2.8 \exp(-18)$	2 614.4
1 %	2.4997 ± 0.0012	0.01994 ± 0.00026	2 541.0
2 %	2.4970 ± 0.0026	0.02027 ± 0.00051	2 632.0
5 %	2.5096 ± 0.0056	0.0213 ± 0.0012	2 636.9
10 %	2.513 ± 0.011	0.0299 ± 0.0023	2 491.1
20 %	2.509 ± 0.017	0.0469 ± 0.0037	2 528.6
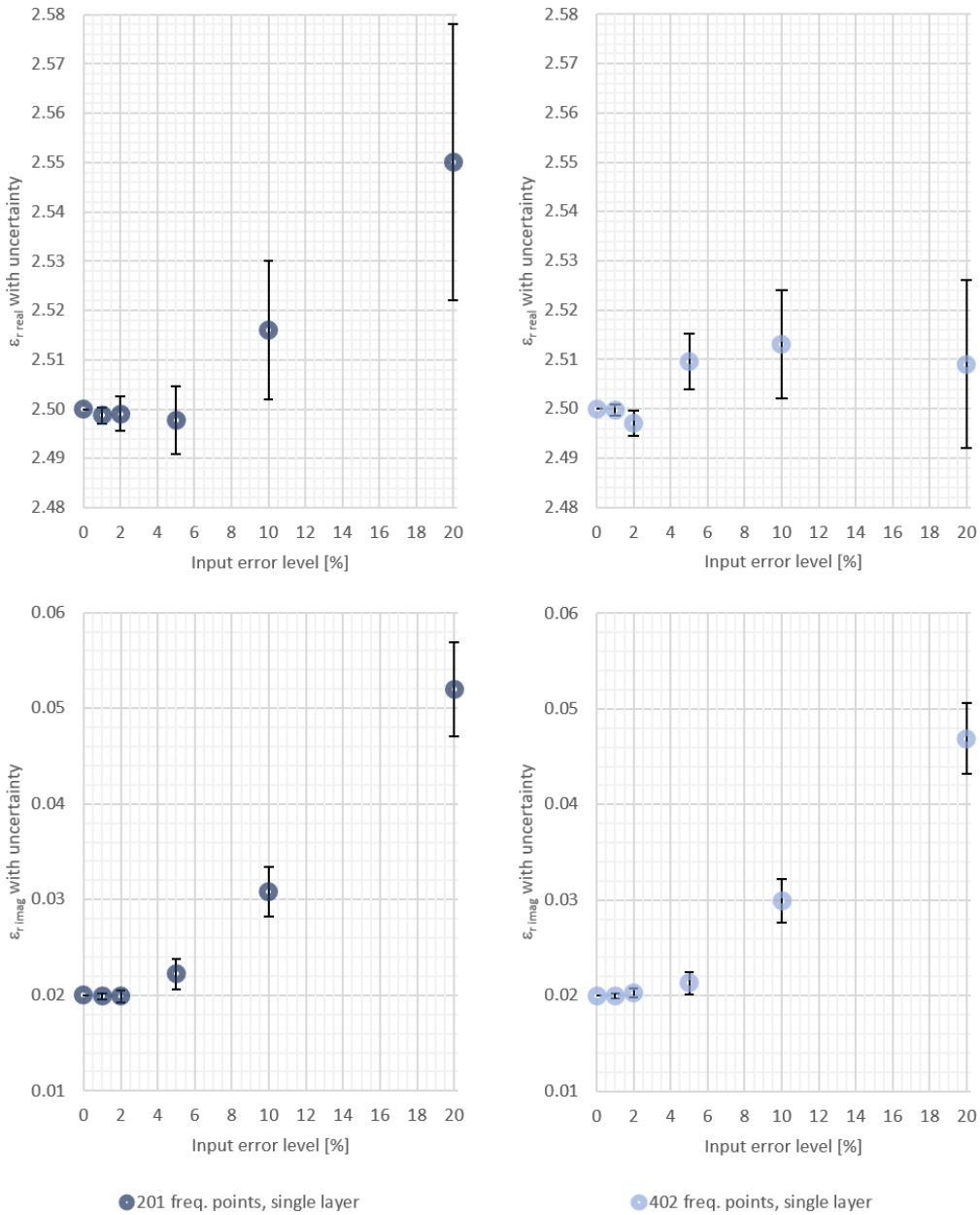
Fig. 7.2 Visualisation of the real and imaginary parts of the complex ϵ_r of a single layer with quantified uncertainties of the test case of 100 repetitions, series of 201 on the left and 402 frequency points on the right

and 1.57mm thick FR-4 has been tested in this experiment. The estimated complex relative permittivities with statistically defined standard uncertainties and analysis of sensitivity on error level of the input data using 201 frequency points is presented in Tab. 7.4. Tab. 7.5 contains results related to 402 frequency points of the input (softer granularity).

The mean values of the real and the imaginary parts of the complex relative permittivity including uncertainties are also depicted in Fig. 7.3.

The softer granularity (higher number of the frequency points) of the input data does not help achieve results noticeably closer to the true values in this case. This result is in contrary with related hypothesis presented in the experimental setup.

7.2.3   A 3-Layered Structure

Finally, a 3-layered structure represents the most complicated case under uncertainty & sensitivity analysis (three pairs of real and imaginary parts of complex relative permittivities what means a six-dimensional optimization problem). The combination of 3.0mm thick PTFE, 1.57mm thick FR-4 and 3.66mm thick plexiglass has been tested in this experiment. The estimated complex relative permittivities with statistically defined standard uncertainties and analysis of sensitivity on error level of the input data using 201 frequency points is presented in Tab. 7.6. Tab. 7.7 contains results related to 402 frequency points of the input.

The mean values of the real and the imaginary parts of the complex relative permittivity including uncertainties are also depicted in Fig. 7.4.

The softer granularity (higher number of the frequency points) helps achieve results closer to the true values in this test rather marginally.

Tab. 7.4 Estimated complex relative permittivity with statistically defined standard uncertainty along with sensitivity analysis on RSD of the error of the input data, a 2-layered structure of PTFE & FR-4, expected $\epsilon_{r_1} = 2.05 - j0.04$ and $\epsilon_{r_2} = 4.2 - j0.084$, 201 frequency points

Noise RSD	$\overline{\epsilon_{r_1\ real}} \pm$ $u_{1\ real}$	$\overline{\epsilon_{r_1\ imag}} \pm$ $u_{1\ imag}$	$\overline{\epsilon_{r_2\ real}} \pm$ $u_{2\ real}$	$\overline{\epsilon_{r_2\ imag}} \pm$ $u_{2\ imag}$	$\overline{t}\ [ms]$
0 %	2.05094 ± 0.00019	0.040422 ± 0.000085	4.19605 ± 0.00079	0.08519 ± 0.00024	6 467.1
1 %	2.0480 ± 0.0018	0.03944 ± 0.00084	4.2048 ± 0.0079	0.0816 ± 0.0024	6 536.1
2 %	2.0486 ± 0.0036	0.0409 ± 0.0017	4.206 ± 0.015	0.0789 ± 0.0046	6 478.0
5 %	2.0544 ± 0.0071	0.0483 ± 0.0042	4.163 ± 0.031	0.0835 ± 0.0080	6 119.0
10 %	2.0728 ± 0.0094	0.0779 ± 0.0092	4.018 ± 0.053	0.109 ± 0.011	6 744.9
20 %	2.088 ± 0.022	0.137 ± 0.016	3.784 ± 0.080	0.122 ± 0.013	5 996.1

Tab. 7.5 Estimated complex relative permittivity with statistically defined standard uncertainty along with sensitivity analysis on RSD of the error of the input data, a 2-layered structure of PTFE & FR-4, expected $\epsilon_{r_1} = 2.05 - j0.04$ and $\epsilon_{r_2} = 4.2 - j0.084$, 402 frequency points

Noise RSD	$\overline{\epsilon_{r_1\ real}} \pm$ $u_{1\ real}$	$\overline{\epsilon_{r_1\ imag}} \pm$ $u_{1\ imag}$	$\overline{\epsilon_{r_2\ real}} \pm$ $u_{2\ real}$	$\overline{\epsilon_{r_2\ imag}} \pm$ $u_{2\ imag}$	$\overline{t}\ [ms]$
0 %	2.05173 ± 0.00060	0.04080 ± 0.00029	4.1928 ± 0.0025	0.08611 ± 0.00069	12 960.5
1 %	2.0485 ± 0.0014	0.03947 ± 0.00061	4.2072 ± 0.0058	0.0813 ± 0.0018	12 919.6
2 %	2.0513 ± 0.0026	0.0415 ± 0.0012	4.192 ± 0.011	0.0849 ± 0.0034	12 946.9
5 %	2.0507 ± 0.0053	0.0443 ± 0.0028	4.188 ± 0.023	0.0801 ± 0.0065	12 879.1
10 %	2.0693 ± 0.0080	0.0649 ± 0.0064	4.082 ± 0.040	0.1002 ± 0.0092	12 812.5
20 %	2.1028 ± 0.0092	0.0990 ± 0.0094	3.923 ± 0.054	0.126 ± 0.011	12 605.0

Fig. 7.3 Visualisation of the real and imaginary parts of the complex ϵ_r of a 2-layered structure with quantified uncertainties of the test case of 100 repetitions, series of 201 on the left and 402 frequency points on the right
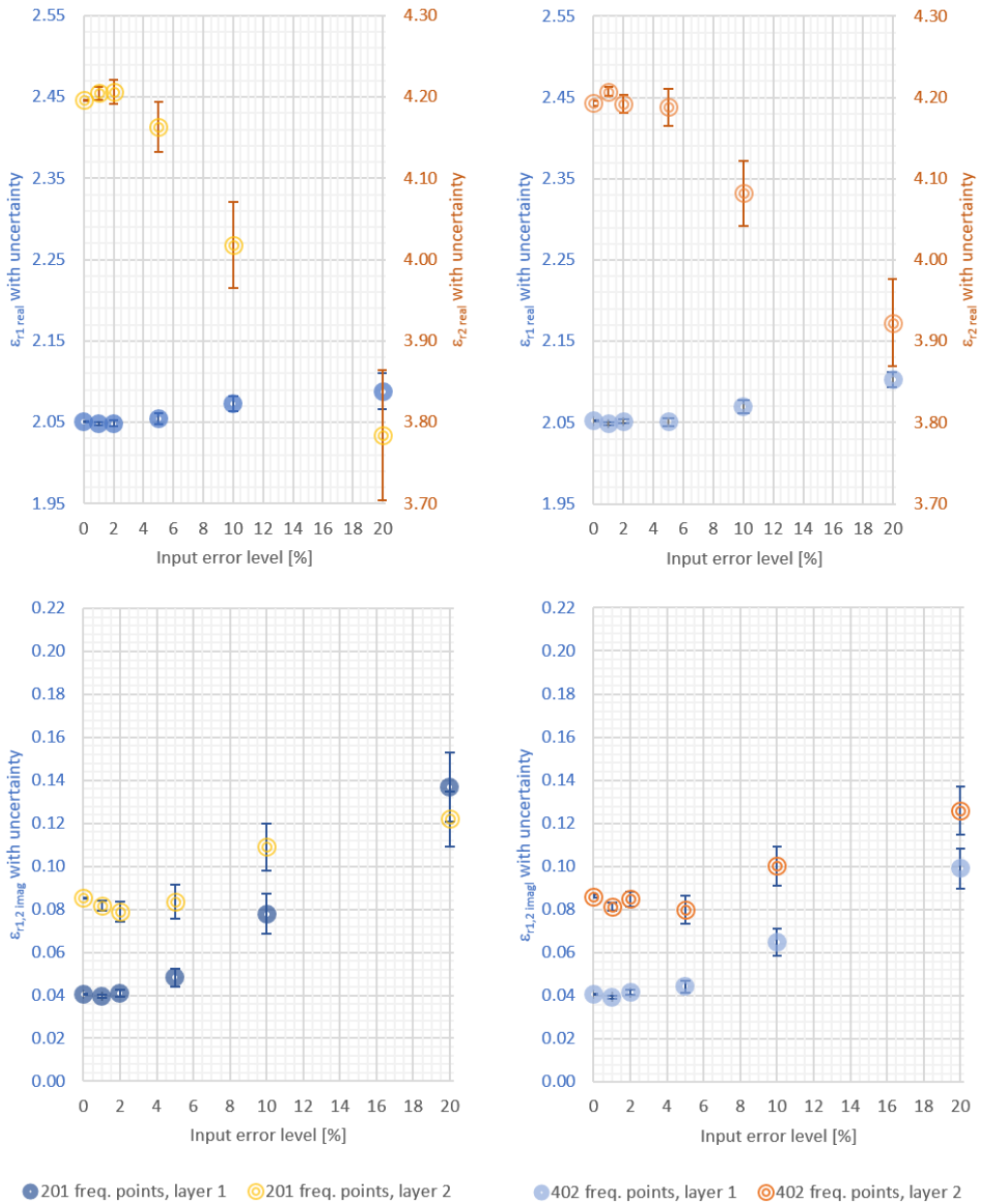
Fig. 7.4 Visualisation of the real and imaginary parts of the complex ϵ_r of a 3-layered structure with quantified uncertainties of the test case of 100 repetitions, series of 201 on the left and 402 frequency points on the right
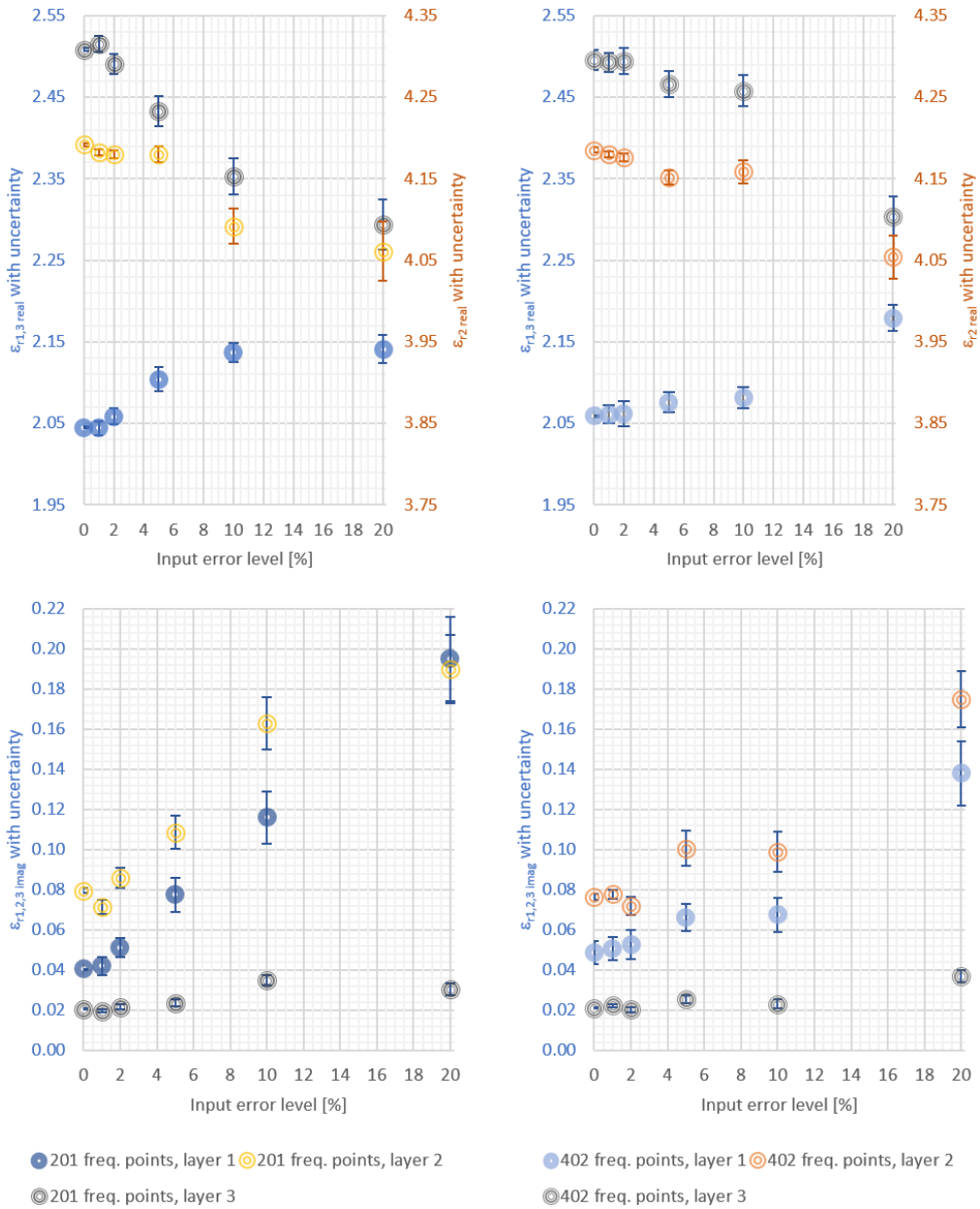
Tab. 7.6 Estimated complex relative permittivity with statistically defined standard uncertainty along with sensitivity analysis on RSD of the error of the input data, a 3-layered structure of PTFE & FR-4 & plexiglass, expected $\epsilon_{r_1} = 2.05 - j0.04$, $\epsilon_{r_2} = 4.2 - j0.084$ and $\epsilon_{r_3} = 2.5 - j0.02$, 201 frequency points

Noise RSD	$\overline{\epsilon_{r_1\ real}}$ $\pm$ $u_{1\ real}$	$\overline{\epsilon_{r_1\ imag}}$ $\pm$ $u_{1\ imag}$	$\overline{\epsilon_{r_2\ real}}$ $\pm$ $u_{2\ real}$	$\overline{\epsilon_{r_2\ imag}}$ $\pm$ $u_{2\ imag}$	$\overline{\epsilon_{r_3\ real}}$ $\pm$ $u_{3\ real}$	$\overline{\epsilon_{r_3\ imag}}$ $\pm$ $u_{3\ imag}$	$\overline{t}\ [ms]$
0 %	2.0450 $\pm$ 0.0013	0.040384 $\pm$ 0.000071	4.1921 $\pm$ 0.0020	0.0796 $\pm$ 0.0011	2.5084 $\pm$ 0.0022	0.02057 $\pm$ 0.00013	13 306.7
1 %	2.0441 $\pm$ 0.0090	0.0419 $\pm$ 0.0044	4.1824 $\pm$ 0.0035	0.0714 $\pm$ 0.0033	2.515 $\pm$ 0.010	0.01952 $\pm$ 0.00086	13 556.8
2 %	2.0586 $\pm$ 0.0095	0.0510 $\pm$ 0.0048	4.1800 $\pm$ 0.0051	0.0858 $\pm$ 0.0049	2.491 $\pm$ 0.012	0.0216 $\pm$ 0.0014	14 203.2
5 %	2.104 $\pm$ 0.015	0.0774 $\pm$ 0.0083	4.1803 $\pm$ 0.0099	0.1086 $\pm$ 0.0084	2.433 $\pm$ 0.019	0.0236 $\pm$ 0.0019	13 768.3
10 %	2.137 $\pm$ 0.012	0.116 $\pm$ 0.013	4.092 $\pm$ 0.022	0.163 $\pm$ 0.013	2.353 $\pm$ 0.022	0.0348 $\pm$ 0.0026	13 881.5
20 %	2.141 $\pm$ 0.017	0.195 $\pm$ 0.021	4.061 $\pm$ 0.036	0.190 $\pm$ 0.017	2.294 $\pm$ 0.031	0.0303 $\pm$ 0.0029	13 614.7

7.3 Summary of the Uncertainty & Sensitivity Analysis

The fact that the deviations from the true (expected) value and uncertainties rise with the RSD of the input error is without a surprise. However, RSD of 20 % of the input error does not lead to similar deviation of the estimations from the expected true value. This relates to the single layer case as well as to the most complicated one represented by a structure containing 3 layers of unknown materials (what means a 6-dimensional MOP).

Considering the simplest case in this section, the single layer with 201 input frequency points, the input error RSD of 20 % resulted in a relative deviation

Tab. 7.7 Estimated complex relative permittivity with statistically defined standard uncertainty along with sensitivity analysis on RSD of the error of the input data, a 3-layered structure of PTFE & FR-4 & plexiglass, expected $\epsilon_{r_1} = 2.05 - j0.04$, $\epsilon_{r_2} = 4.2 - j0.084$ and $\epsilon_{r_3} = 2.5 - j0.02$, 402 frequency points

Noise RSD	$\epsilon_{r_1\ real}$ ± $u_{1\ real}$	$\epsilon_{r_1\ imag}$ ± $u_{1\ imag}$	$\epsilon_{r_2\ real}$ ± $u_{2\ real}$	$\epsilon_{r_2\ imag}$ ± $u_{2\ imag}$	$\epsilon_{r_3\ real}$ ± $u_{3\ real}$	$\epsilon_{r_3\ imag}$ ± $u_{3\ imag}$	$\bar{t}$ [ms]
0 %	2.0589 ± 0.0011	0.0487 ± 0.0057	4.1854 ± 0.0034	0.0764 ± 0.0017	2.496 ± 0.012	0.02109 ± 0.00026	27 655.1
1 %	2.061 ± 0.011	0.0508 ± 0.0058	4.1797 ± 0.0036	0.0778 ± 0.0023	2.493 ± 0.012	0.02212 ± 0.00054	27 533.2
2 %	2.062 ± 0.015	0.0527 ± 0.0074	4.1762 ± 0.0047	0.0720 ± 0.0046	2.495 ± 0.016	0.0203 ± 0.0012	27 318.6
5 %	2.076 ± 0.012	0.0662 ± 0.0066	4.1522 ± 0.0088	0.1006 ± 0.0086	2.466 ± 0.016	0.0255 ± 0.0019	27 017.4
10 %	2.082 ± 0.013	0.0675 ± 0.0084	4.159 ± 0.014	0.099 ± 0.010	2.458 ± 0.019	0.0231 ± 0.0022	26 745.0
20 %	2.179 ± 0.016	0.138 ± 0.016	4.054 ± 0.027	0.175 ± 0.014	2.304 ± 0.024	0.0369 ± 0.0030	27 186.5

of 2.02 % of the final estimated mean (comparing the absolute values of the estimated mean and the true complex relative permittivity). This is a good result. However, it is even much better in the case of 402 input frequency points (as expected). The deviation is only 0.37 % in this case.

Considering the most complicated case of 3-layered structure, again, comparing the absolute values of complex relative permittivities of the estimated mean and the true value (in the case of the input error with RSD of 20 %) the results are acceptable. The relative deviation of the final estimations is 4.85 %, 3.22 % and 8.23 % (for the first, the second and the third layer respectively) in the case of 201 frequency points in the input. Running the software with 402 input

frequency points it results in 6.49 %, 3.41 % and 7.83 %. Therefore, this is an example in which the softer granularity of the input data did not lead to results closer to the true value. From the pragmatical point of view, it is still surprising that the software can achieve reasonable results at all considering the high dimensionality of the problem.

Impact of the granularity of measurement is mainly visible only in the single layer case. It may be well understandable in the visualization of the results including uncertainties (Fig. 7.2). The resulting mean value is usually more close to the true value when working with softer granularity of the input data (402 frequency points). Also the standard uncertainty of the mean is lower. However, there is no impact of double number of frequency points or rather marginal in the 3-layered structure case.

The processing time expands from at about 1.3 second in the single layer case to at about 13 seconds in the case of the 3-layered structure (when working with 201 frequency points in both cases). Therefore, solving the more difficult case (3 layers) is approximately 10-times slower then the processing of the simple case (1 layer) what still can be considered as a good result taking into account the difference between the dimensionality of the searched spaces: two versus six dimensions.

Additional two purely statistical notes about the background of the analyses provided in this section follows:

- The total number of test executions of the software for the purpose of creation this uncertainty & sensitivity analysis can be stated simply: 6 levels of RSD of the input data × 2 granularities of the input data × 3 different numbers of layers × 100 repetitions. This is equal to 3 600 runs of the software in total.

- The total processing time of all the test runs of the software is 38 479.74 seconds what means 10 hours, 41 minutes and nearly 20 seconds of sequential testing without any pause (on a particular computer described in subsection 6.3).

8   CONCLUSIONS AND FUTURE RESEARCH DIRECTIONS

This section summarizes the approach, achieved goals and results of the experiments presented in the thesis, including the summary of the specific solution and contributions. Ultimately, possible directions for future work are also mentioned.

8.1   Summary

This doctoral thesis describes a specific approach aimed at estimation of complex permittivity of single or multi-layered structures. Its processing is based on data obtained by measuring the transmission and reflection coefficients using horn antennas in free space in the frequency range above 1 GHz. The proposed solution is presented by a working combination of a direct model computing transmission and reflection coefficients from known permittivity of layered structure under test and the Particle Swarm Optimization. This method has not yet been presented in the contemporary scientific literature, it is unusual and quite difficult to arrange due to the inverse (and thus non-deterministic) nature of this problem.

The direct mathematical model in combination with the selected evolutionary algorithm plays a significant role in the whole system and makes it possible to estimate complex permittivity of materials in multi-layered structures. This system provides reasonable estimations of permittivity. Moreover, the speed of the system implemented in C++ is rather fast.

The reflection of the research objectives follows:

- A direct mathematical model computing reliable S-parameters of a known material and of a multi-layered structure of materials in free space at specific frequency ranges has been designed on the basis of the up-to-date scientific publications available at the moment.

- The direct mathematical model has been implemented into a software using C++.

- The direct mathematical model has been verified by comparing its synthetic data and data obtained by direct measurements.

- An EA (PSO) has been implemented into the software and combined with the direct mathematical model.

- Many experiments with synthetic data and real (measured) data were performed; said experiments confirm the ability of the developed system to estimate complex relative permittivity of unknown single and multi-layered structures.

- The uncertainty analysis along with the sensitivity analysis of the software has been elaborated and presented in the form of tables and figures.

In conclusion, the doctoral thesis fulfils all the required objectives.

8.2   Contributions

Nowadays, the way of how to compute the transmission and reflection coefficients of a known non-magnetic homogeneous isotropic material (or several layers of known materials) at specific frequency range is already known and documented. Work presented in this thesis is based on this knowledge and the inner direct model of designed system is based on it. This direct model in combination with PSO produces reasonable estimations of complex permittivity with rather low uncertainties and low sensitivity on the error of the input data. This is a non-trivial inverse task which is not presented yet in the science to date as far as the author knows. Therefore, the novel approach presented in this work may be evaluated as contributive to science also with respect to the functional and verified implementation of the designed system.

The designed system implemented into a functional software is one of the main contributions of this work. The executable binary files together with the source codes and the software documentation are attached (see Appendix A).

Another remarkable innovation in this work is the move in frequency band used for measuring and processing. This area (millimetre and sub-millimetre waves)

is new also for known materials what means another breakthrough. Shift in frequencies brings also some complications. One of them is the resonance. For example the resonance of the molecules of water vapour appears near 183.310 GHz [24, 40].

It is expectable that the approaches designed in the doctoral thesis may be acknowledged primarily in the area of material physics and electrotechnics. However, it may be also applicable in the remote measurements, analysis of materials in cosmos (like measuring the thickness of specific materials, glaciers for instance) what represents a great potential of impact.

This type of research may become important in the industry in the near future for its capability to estimate properties of very new materials. This is also the area where the Department of Electronics and Measurement of Tomas Bata University in Zlín may have a chance to contribute and play an important role in terms of its laboratories' equipment and expert staff with up-to-date know-how.

8.3 Future Research Directions

The results of experiments that were based on synthetic data are very promising. However, the final estimations of permittivity in case of experiments that were based on data obtained by direct measurements were, in some cases, not so convincing. Therefore, future research should focus on a wider set of direct measurements to check (and possibly improve) the estimation behaviour of the complex relative permittivity.

Nevertheless, real data obtained by direct measurements are not the only thing on which the further improvements of the system may be based. Utilization of a simulation software producing relevant S-parameters, such as CST Studio Suite (3D electromagnetic field simulation and analysis software [1]) or Microwave Office (circuit design software that delivers accurate simulation for RF/microwave product development [12]), would be also beneficial. Such software may produce quantity (numerous multi-layered structures) along with quality with respect to the need of reliable S-parameters used as the test system input.

REFERENCES

[1] 3DEXPERIENCE® COMPANY - DASSAULT SYSTÈMES®. CST Studio Suite 3D EM simulation and analysis software [online]. https://www.3ds.com/products-services/simulia/products/cst-studio-suite/, 2020. [cit. 2020-01-26].

[2] Agilent Technologie. Agilent 2-Port PNA-L MicrowaveNetwork Analyzer. Technical report, Agilent Technologies, Inc., 2011.

[3] ALEXNLD. FR4 Fibreglass Sheet 300 150mm [online]. https://alexnld.com/product/glassfibre-sheet-grp-epoxy-glass-fr4-fibreglass-sheet-300-150mm/, 2020. [cit. 2020-01-24].

[4] AVKO. Expanded PTFE tape [online]. http://www.avko.eu/english/products/expanded-ptfe-products/expanded-ptfe-tape, 2012. [cit. 2018-02-14].

[5] BABA, N. H., AWANG, Z. and GHODGAONKAR, D. K. A free-space method for measurement of complex permittivity of silicon wafers at microwave frequencies. In *Applied Electromagnetics, 2003. APACE 2003. Asia-Pacific Conference on*, pp. 119–123. IEEE, August 2003. ISBN 0-7803-8129-7.

[6] BAKER-JARVIS, J., VANZURA, E. J. and KISSICK, W. A. Improved technique for determining complex permittivity with the transmission/reflection method. *Microwave Theory and Techniques, IEEE Transactions on*. August 1990, 38, 8, pp. 1096–1103. ISSN 0018-9480.

[7] BELL, S. *A Beginner's Guide to Uncertainty of Measurement*. Measurement good practice guide. National Physical Laboratory, 11 (issue 2) edition, 2001.

[8] BONAGUIDE, G. and JARVIS, N. *The VNA Applications Handbook*. Artech House microwave library. Artech House, 2019. ISBN 9781630816025.

[9] BOUKHATER, C., DAKROUB, O., LAHOUD, F., AWAD, M. and ARTAIL, H. An intelligent and fair GA carpooling scheduler as a social solution for greener transportation. In *Proceedings of the Mediterranean Electrotechnical*

Conference - MELECON, pp. 182–186, 04 2014. doi: 10.1109/MELCON. 2014.6820528. ISBN 978-1-4799-2337-3.

[10] BOURREAU, D., PEDEN, A. and MAGUER, S. L. A Quasi-Optical Free-Space Measurement Setup Without Time-Domain Gating for Material Character-ization in the W-Band. *Instrumentation and Measurement, IEEE Transac-tions on*. December 2006, 55, 6, pp. 2022–2028. ISSN 0018-9456.

[11] BRACHTENDORF, K. Minimize Mathematical Function Rastrigin Part 1 [online]. https://github.com/KilianB/Darwin/wiki/0.-Minimize-Mathema-tical-Function-Rastrigin-Part-1, 2018. [cit. 2020-01-26].

[12] CADENCE DESIGN SYSTEMS, INC. Microwave Office AWR Software [online]. https://www.awr.com/software/products/microwave-office, 2020. [cit. 2020-01-26].

[13] COELLO, C. A. C., LAMONT, G. L. and VELDHUIZEN, D. A. *Evolutionary Algorithms for Solving Multi-Objective Problems*. Genetic and Evolutionary Computation. Springer, 2nd edition, 2007. doi: 10.1007/978-0-387-36797-2.

[14] DANIDEH, A. and NEUESTANAK, A. A. L. CPW Fed Double T-Shaped Array Antenna with Suppressed Mutual Coupling. *International Journal of Communications, Network and System Sciences*. 2010, 3, pp. 190–195. doi: 10.4236/ijcns.2010.32027.

[15] DELORME, A. *Statistical Methods*, 6, pp. 240–264. Wiley interscience, 2006. doi: 10.1002/0471732877.emd318. ISBN 9780471732877.

[16] DEPARTMENT OF DIELECTRICS. Laboratory of Terahertz Spectroscopy, Prague [online]. https://lts.fzu.cz/en/res-thz.htm, 2016. [cit. 2016-11-28].

[17] DJORDJEVIC, A. R., BILJIE, R. M., LIKAR-SMILJANIC, V. D. and SARKAR, T. K. Wideband frequency-domain characterization of FR-4 and time-domain causality. *IEEE Transactions on Electromagnetic Compatibility*. Nov 2001, 43, 4, pp. 662–667. ISSN 1558-187X. doi: 10.1109/15.974647.

[18] ELHAWIL, A., ZHANG, L., STIENS, J., TANDT, C. D., GOTZEN, N. A., ASSCHE, G. V. and VOUNCKX, R. A Quasi-Optical Free-Space Method

for Dielectric Constant Characterization of Polymer Materials in mm-wave Band. In *Proceedings Symposium IEEE/LEOS Benelux Chapter*, pp. 187–190, 2007.

[19] EVERYTHING RF. Waveguide Sizes [online]. http://www.everythingrf.com/tech-resources/waveguides-sizes, 2013. [cit. 2014-12-26].

[20] FIX, J. POPulation based Optimization Toolbox [online]. https://github.com/jeremyfix/popot/, 2016. [cit. 2020-01-20].

[21] FRALICK, D. T. W-band Free Space Permittivity Measurement Setup for Candidate Radome Materials. Technical report, NASA Langley Technical Report Server, 1997.

[22] FRIEDSAM, G. L. and BIEBL, E. M. A broadband free-space dielectric properties measurement system at millimeter wavelengths. In *Precision Electromagnetic Measurements Digest, 1996 Conference on*, pp. 210–211, June 1996.

[23] GAGNON, N., SHAKER, J., BERINI, P., ROY, L. and PETOSA, A. Material characterization using a quasi-optical measurement system. *Instrumentation and Measurement, IEEE Transactions on*. April 2003, 52, 2, pp. 333–336. doi: 10.1109/TIM.2003.810042. ISSN 0018-9456.

[24] GAUT, N. E. Studies of atmospheric water vapor by means of passive microwave techniques. Technical report, MIT Research Laboratory of Electronics, 1968.

[25] GHODGAONKAR, D. K., VARADAN, V. V. and VARADAN, V. K. Free-space measurement of complex permittivity and complex permeability of magnetic materials at microwave frequencies. *Instrumentation and Measurement, IEEE Transactions on*. April 1990, 39, 2, pp. 387–394. ISSN 0018-9456.

[26] GROSVENOR, C. A., JOHNK, R. T., BAKER-JARVIS, J., JANEZIC, M. D. and RIDDLE, B. Time-Domain Free-Field Measurements of the Relative Permittivity of Building Materials. *Instrumentation and Measure-*

ment, IEEE Transactions on. July 2009, 58, 7, pp. 2275–2282. doi: 10.1109/TIM.2009.2013916. ISSN 0018-9456.

[27] HADDAD, O. B., AFSHAR, A. and MARIŇO, M. A. Honey-Bees Mating Optimization (HBMO) Algorithm: A New Heuristic Approach for Water Resources Optimization. *Water Resources Management.* October 2006, 20, 5, pp. 661–680. ISSN 1573-1650. doi: 10.1007/s11269-005-9001-3.

[28] HALLIDAY, D., RESNICK, R. and WALKER, J. *Fundamentals of Physics.* John Wiley & Sons, Inc., 5th edition, 1997. ISBN 9780471283232.

[29] HASHIMOTO, O., SATO, A., HANAZAWA, M., TANI, K. and ENDO, T. A study on measurement of dielectric constant by free space transmission method at C band. *Electronics and Communications in Japan (Part I: Communications).* 2004, 87, 10, pp. 18–25. doi: 10.1002/ecja.10191. ISSN 1520-6424.

[30] HORÁK, T., MASTORAKIS, N. and LÁNSKÁ, M. Report on Recent Scientific Applications of Self-Organizing Migration Algorithm. In *Proceedings of the 12th WSEAS International Conference on Applied Informatics and Communications (AIC '12)*, pp. 247–251, Istanbul, Turkey, 2012. ISBN 978-1-6180-4113-5.

[31] HUDLIČKA, M. and KAZEMIPOUR, A. Určování materiálových parametrů ve volném prostoru. In *39. pravidelné setkání zájemců o mikrovlnnou techniku*, Prague, the Czech Republic, 2013. Česká elektrotechnická společnost, z. s. ISBN 978-80-02-02488-0.

[32] JOHNSON, J. M. and RAHMAT-SAMII, V. Genetic Algorithms in Engineering Electromagnetics. *IEEE Antennas and Propagation Magazine.* Aug 1997, 39, 4, pp. 7–21. ISSN 1558-4143. doi: 10.1109/74.632992.

[33] JUDISH, R. M. and SPLETT, J. Robust statistical analysis of vector network analyzer intercomparisons. In *IMTC/99. Proceedings of the 16th IEEE Instrumentation and Measurement Technology Conference (Cat. No.99CH36309)*, 3, pp. 1320–1324, May 1999. doi: 10.1109/IMTC.1999.776019.

[34] KEINER, L. E. Electromagnetic spectrum [online]. http://en.citizendium. org/wiki/File:Electromagnetic-Spectrum.png, 2009. [cit. 2014-12-25].

[35] KENNEDY, J. and EBERHART, R. Particle swarm optimization. In *IEEE International Conference on Neural Networks*, 4, pp. 1942–1948. IEEE, 1995.

[36] KŘESÁLEK, V. and NAVRÁTIL, M. Estimation of complex permittivity using evolutionary algorithm from measured data of reflectance and transmittance in free space. *Microwave and Optical Technology Letters*. 2015, 57, 7, pp. 1542–1546. doi: 10.1002/mop.29135.

[37] KOMAROV, V., WANG, S. and TANG, J. Permittivity and Measurements. In CHANG, K. (Ed.) *Encyclopedia of RF and Microwave Engineering*. : John Wiley & Sons, Inc., 2005. ISBN 978-0-471-27053-9.

[38] KUMAR, S. B., RAVEENDRANATH, U., MOHANAN, P., MATHEW, K. T., HAJIAN, M. and LIGTHART, L. P. A simple free-space method for measuring the complex permittivity of single and compound dielectric materials. *Microwave and Optical Technology Letters*. 2000, 26, 2, pp. 117–119. doi: 10. 1002/1098-2760(20000720)26:2<117::AID-MOP14>3.0.CO;2-I. ISSN 1098-2760.

[39] LEŚNIKOWSKI, J. Dielectric permittivity measurement methods of textile substrate of textile transmission lines. *Przegląd Elektrotechniczny*. 2012, R. 88, nr 3a, pp. 148–151.

[40] MATSUSHITA, S. and MATSUO, H. *Relation between 183 GHz Water Vapor Line and Water Continuum Absorption Measured with FTS*, 266 / *Astronomical Society of the Pacific Conference Series*, pp. 180–187. Astronomical Society of the Pacific, January 2002.

[41] METAXAS, A. C. and MEREDITH, R. J. *Industrial Microwave Heating*. Energy Engineering Series. P. Peregrinus, 1983. ISBN 9780906048894.

[42] MITCHELL, M. *An Introduction to Genetic Algorithms*. MIT Press, 1998. ISBN 0262631857.

[43] NAKHKASH, M., HUANG, Y., AL-NUAIMY, W. and FANG, M. T. C. An improved calibration technique for free-space measurement of complex permittivity. *Geoscience and Remote Sensing, IEEE Transactions on*. February 2001, 39, 2, pp. 453–455. doi: 10.1109/36.905254. ISSN 0196-2892.

[44] ONWUBOLU, G. C. and BABU, B. V. *New optimization techniques in engineering*. Springer, 2004. ISBN 978-3-540-39930-8.

[45] ORLOB, C., REINECKE, T., DENICKE, E., GECK, B. and ROLFES, I. Compact Unfocused Antenna Setup for X-Band Free-Space Dielectric Measurements Based on Line-Network-Network Calibration Method. *Instrumentation and Measurement, IEEE Transactions on*. July 2013, 62, 7, pp. 1982–1989. doi: 10.1109/TIM.2013.2246905. ISSN 0018-9456.

[46] PARSONS, H. M., EKMAN, D. R., COLLETTE, T. W. and VIANT, M. R. Spectral Relative Standard Deviation: A Practical Benchmark in Metabolomics. *Analyst*. 2009, 134, pp. 478–485. doi: 10.1039/B808986H.

[47] PATEL, J. and READ, C. *Handbook of the Normal Distribution, Second Edition*. Statistics: A Series of Textbooks and Monographs. Taylor & Francis, 1996. ISBN 9780824793425.

[48] PATNAIK, P. and (FIRM), K. *Handbook of Inorganic Chemicals*. McGraw-Hill handbooks. McGraw-Hill, 2003. ISBN 9780070494398.

[49] PERINI, J. and COHEN, L. S. Design of broad-band radar-absorbing materials for large angles of incidence. *IEEE Transactions on Electromagnetic Compatibility*. May 1993, 35, 2, pp. 223–230. ISSN 0018-9375. doi: 10.1109/15.229418.

[50] POINERN, G., ALI, N. and FAWCETT, D. Progress in Nano-Engineered Anodic Aluminum Oxide Membrane Development. *Materials*. 2011, 4, 3, pp. 487–526. ISSN 1996-1944. doi: 10.3390/ma4030487.

[51] RAJAB, K., NAFTALY, M., LINFIELD, E., NINO, J., ARENAS, D., TANNER, D., MITTRA, R. and LANAGAN, M. Broadband Dielectric Characterization of Aluminum Oxide (Al 2 O 3). *Journal of Microelectronics and Electronic Packaging*. 01 2008, 5, pp. 2–7. doi: 10.4071/1551-4897-5.1.1.

[52] RAO, C. R. *Karl Pearson Chi-Square Test The Dawn of Statistical Inference*, pp. 9–24. Birkhäuser Boston, Boston, MA, 2002. doi: 10.1007/978-1-4612-0103-8_2. ISBN 978-1-4612-0103-8.

[53] RIDDLE, B., BAKER-JARVIS, J. and KRUPKA, J. Complex permittivity measurements of common plastics over variable temperatures. *Microwave Theory and Techniques, IEEE Transactions on*. March 2003, 51, 3, pp. 727–733. doi: 10.1109/TMTT.2003.808730. ISSN 0018-9480.

[54] Rogers Corporation. RO4003®, RO4350® High Frequency Laminates. Technical report, Rogers Corporation, Microwave Materials Division, 1999.

[55] RYYNÄNEN, S. The electromagnetic properties of food materials: A review of the basic principles. *Journal of Food Engineering*. 1995, 26, 4, pp. 409–429. ISSN 0260-8774. doi: 10.1016/0260-8774(94)00063-F.

[56] SASAKI, K., SEGAWA, H., MIZUNO, M., WAKE, K., WATANABE, S. and HASHIMOTO, O. Development of the complex permittivity measurement system for high-loss biological samples using the free space method in quasi-millimeter and millimeter wave bands. *Physics in Medicine and Biology*. 2013, 58, 5, pp. 1625–1633. doi: 10.1088/0031-9155/58/5/1625.

[57] STOCK, M., DAVIS, R., MIRANDÉS, E. and MILTON, M. J. T. The revision of the SI—the result of three decades of progress in metrology. *Metrologia*. February 2019, 56, 2, pp. 022001. doi: 10.1088/1681-7575/ab0013.

[58] STROUSTRUP, B. *A Tour of C++*. Addison-Wesley, 2nd edition, 2018. ISBN 978-0-13-499783-4.

[59] TAP PLASTICS. Cast Acrylic Sheets Cut-To-Size [online]. https://www.tapplastics.com/product/plastics/cut_to_size_plastic/acrylic_sheets_cast_clear/510, 2020. [cit. 2020-01-24].

[60] HIPPEL, A. R. *Dielectrics and Waves*. Wiley, 1954.

[61] HIPPEL, A. R. *Dielectric materials and applications*. M.I.T. Press, 1961.

[62] WANG, D., TAN, D. and LIU, L. Particle swarm optimization algorithm: an overview. *Soft Computing*. Jan 2018, 22, 2, pp. 387–408. ISSN 1433-7479. doi: 10.1007/s00500-016-2474-6.

[63] WEBSTER, J. *Electrical Measurement, Signal Processing, and Displays*. Principles and Applications in Engineering. CRC Press, 2003. ISBN 9780203009406.

[64] WEE, F. H., SOH, P. J., SUHAIZAL, A. H. M., NORNIKMAN, H. and EZANUDDIN, A. A. M. Free space measurement technique on dielectric properties of agricultural residues at microwave frequencies. In *Microwave and Optoelectronics Conference (IMOC), 2009 SBMO/IEEE MTT-S International*, pp. 183–187, November 2009. doi: 10.1109/IMOC.2009.5427603. ISSN 1679-4389.

[65] YANG, X. *Appendix A: Test Problems in Optimization*, pp. 261–266. John Wiley & Sons, Inc., July 2010. doi: 10.1002/9780470640425. ISBN 978-0-470-58246-6.

[66] ZAKI, F. A. M., AWANG, Z., BABA, N. H., ZOOLFAKAR, A. S., BAKAR, R. A., ZOLKAPLI, M. and FADZLINA, N. A free-space method for measurement of complex permittivity of double-layer dielectric materials at microwave frequencies. In *Research and Development (SCOReD), 2010 IEEE Student Conference on*, pp. 12–15, December 2010. doi: 10.1109/SCORED.2010.5703961.

[67] ZELINKA, I. *SOMA – Self-Organizing Migrating Algorithm*, pp. 167–217. Springer Berlin Heidelberg, Berlin, Heidelberg, 2004. doi: 10.1007/978-3-540-39930-8_7. ISBN 978-3-540-39930-8.

PUBLICATIONS OF THE AUTHOR

[P.1] Tomášek, P., Fredouille, C. and Matrouf, D. Factor analysis-based approaches applied to the speaker diarization task of meetings: a preliminary study, In *Proceedings of the Speaker and Language Recognition Workshop*. Speaker Odyssey 2010, Brno, the Czech Republic, 2010.

[P.2] Tomášek, P., Křesálek, V. and Goňa, S. Přehled čtyř moderních metod z oblasti evolučních algoritmů využitelných v optice, *Jemná mechanika a optika*. 2012, issue 9, pp. 244–248. ISSN 0447-6441.

[P.3] Tomášek, P. Optimalizovaný Bluetooth FSS filtr, *iDB Journal*. 2013, issue 4, pp. 47–48. ISSN 1338-3337.

[P.4] Goňa, S., Tomášek, P. and Křesálek, V. Automatizovaný návrh kvazioptických filtrů na milimetrových vlnách v Matlabu, *Jemná mechanika a optika*. 2013, issue 7-8, pp. 219–222. ISSN 0447-6441.

[P.5] Goňa, S., Tomášek, P. and Křesálek, V. Measurement of Conductivity of Carbon Fibers at Microwave Frequencies, In *23rd International Conference Radioelektronika*. New York: IEEE, 2013, pp. 68–71. ISBN 978-1-4673-5516-2.

[P.6] Tomášek, P. and Shestopalov, Yu V. Parameter optimization of waveguide filters employing analysis of closed-form solution, In *Progress in Electromagnetics Research Symposium*. Cambridge: Electromagnetics Academy, 2013, pp. 296–299. ISSN 1559-9450. ISBN 9781934142264.

[P.7] Tomášek, P. and Goňa, S. Automated design of frequency selective surfaces with the application to Wi-Fi band-stop filter, In *Progress in Electromagnetics Research Symposium*. Cambridge: Electromagnetics Academy, 2013, pp. 221–224. ISSN 1559-9450. ISBN 9781934142264.

[P.8] Tomášek, P. and Shestopalov, Yu V. Parameter Optimization

of Waveguide Filters, In *RADIOINFOKOM – 2013*. Moscow, Russia: MIREA Bauman, 2013, pp. 259–263. ISBN UDK621.396.

[P.9]   TOMASEK, P. Open Source Software for Engineers, In *3mi*. VŠB TU, Ostrava, 2013, pp. 194–197. ISBN 978-80-248-3233-3.

[P.10]   TOMASEK, P. Automated Design of 5 GHz Wi-Fi FSS Filter, In *Advances in Intelligent Systems and Computing* (Former Name: *Advances in Soft Computing*). 2014, Volume 285, Springer, pp. 313–319. ISSN: 2194-5357.

[P.11]   TOMASEK, P. Analysis of Materials Based on Inverse Modeling, In *ICAMSME 2014, Advanced Material Research*. Trans Tech Publications, ISSN: 1662-8985.

[P.12]   TOMASEK, P. Source Reconstruction of Electromagnetic Fields Employing Modern Evolutionary Algorithms, *International Journal of Mathematical Models and Methods in Applied Sciences*. 2014, Volume 8, pp. 429–433, ISSN: 1998-0140.

[P.13]   TOMASEK, P. Optimization of FSS Filters, *International Journal of Circuits, Systems and Signal Processing*. 2014, Volume 8, pp. 594–599, ISSN: 1998-4464.

[P.14]   TOMASEK, P. and SHESTOPALOV, Yu V. Verification of Computational Model of Transmission Coefficients of Waveguide Filters, In *PIERS Proceedings* 2015, Prague, Czech Republic, pp. 1538–1541. ISBN: 978-1-934142-30-1.

[P.15]   TOMASEK, P., SHESTOPALOV, V. and KŘESÁLEK, V. Comparison of Selected Evolutionary Techniques Used in Estimation of Permittivity, In *Proceedings of the 2015 ICEAA* Torino, Italy, pp. 614–617. ISBN: 978-1-4799-7805-2.

[P.16]   TOMASEK, P., SHESTOPALOV, V. and KŘESÁLEK, V. Reconstruction of Permittivity of Multiple Layers in Free-Space, In *Proceedings of the 2015 ICEAA*, Torino, Italy, pp. 610–613. ISBN: 978-1-4799-7805-2.

[P.17] TOMASEK, P. Reconstruction of Permittivity of Unknown Materials in Free Space, In *17th International Carpathian Control Conference (ICCC)*, Tatranská Lomnica, Slovak Republic, 2016, pp. 743–746, ISBN: 978-1-4673-8605-0.

[P.18] TOMASEK, P. Attenuation of Wireless Communication under IEEE 802.11ah, *Annals of DAAAM International 2016*, Volume 27, No.1, ISSN 2304-1382, ISBN 978-3-902734-13-6, CDROM version, Ed. B. Katalinic, Published by DAAAM International, Vienna, Austria, EU, 2016, DOI:10.2507/27th.daaam.proceedings.xxx.

[P.19] TOMASEK, P. Estimation of Permittivity of Materials using Sub-Millimeter Waves. In *18th International Carpathian Control Conference (ICCC)*, Sinaia, Romania, 2017, ISBN: 978-1-5090-5825-9.

[P.20] MACH, V., ADÁMEK, M., VALOUCH, J. and TOMÁŠEK, P. Software Extension for Advanced Technology Zone, *29th DAAAM International Symposium on Intelligent Manufacturing and Automation*, Zadar, 2018, DOI: 10.2507/29th.daaam.proceedings.xxx.

[P.21] VASKOVA, H., TOMASEK, P. and STRUSKA, M. Application of Raman spectroscopic measurement for banknote security purposes, *3rd International Conference on: Applied Physics, System Science and Computer*, Dubrovnik, 2018.

[P.22] TOMASEK, P. On the use of Evolutionary Algorithms in Estimation of Permittivity. In *19th International Carpathian Control Conference (ICCC)*, Szilvásvárad, Hungary, 2018, ISBN: 978-1-5386-4761-5, Publisher: IEEE. DOI: 10.1109/CarpathianCC.2018.8399596.

CURRICULUM VITAE

This section includes some general information about the author along with more details about his educational background and work experiences.

General

Name and surname:	Pavel Tomášek
Date of birth:	2nd December 1985
Gender:	Male
Nationality:	Czech
Address:	Nádražní 390, 768 05 Koryčany, the Czech Republic
E-mail:	tomasek@utb.cz

Education and Training

Since September 2011: *doctoral degree study programme* (Engineering Informatics, P3902, ISCED 6), Tomas Bata University in Zlín, Faculty of Applied Informatics, Nad Stráněmi 4511, 760 05 Zlín, the Czech Republic, activities:

- Freemover internship at Slovak University of Technology in Bratislava, Faculty of Mechanical Engineering (the Slovak Republic, 2018), solving the inverse problem of the doctoral thesis, programming in C++,

- Freemover internship at University of the Peloponnese (Greece, 2015), solving inverse problems, programming in MatLAB,

- Freemover internship at Karlstad University (Sweden, 2012): numerical analysis, inverse problems, optimization, project: "Parameter Optimization of Filters Employing Multi-Sectional Diaphragms in Waveguides of Rectangular Cross Section",

- teaching: super-standard components of object security, introduction to LaTeX,

- creation of LaTeX templates of bachelor's thesis, master's thesis, doctoral thesis, treatise on doctoral thesis, doctoral thesis statement and habilitation thesis statement for all the faculties of Tomas Bata University in Zlín,

- project participations:

  - 06/3/2018/GAMA TG03010052 – National database for camera trap records (analysis and realization of a prototype), and
  - MPO-DENESA-TRIO-FV20419 – Computer vision software for automatic sorting of saplings' seedlings.

September 2008 – June 2011: *subsequent full-time master's study programme* (Computer Graphics and Multimedia, N2646, ISCED 5A), Brno University of Technology, Faculty of Information Technology, Božetěchova 2, 612 66 Brno, the Czech Republic, Socrates Erasmus internship in Laboratoire Informatique d'Avignon (France, 2009-2010, programming a speech processing software [A.1]),

February 2009 – November 2010: *supplementary pedagogical study* (ISCED 5A), Brno University of Technology, Faculty of Electrical Engineering and Communication, Technická 3058/10, 616 00 Brno, the Czech Republic,

September 2005 – June 2008: *full-time bachelor study programme* (Information Technology, B2646, ISCED 5A), Brno University of Technology, Faculty of Information Technology, Božetěchova 2, 612 66 Brno, the Czech Republic,

September 1997 – June 2005: *grammar school* (ISCED 3A), Klvaňovo gymnázium v Kyjově, Komenského 549, 697 11 Kyjov, the Czech Republic, graduation certificate, passed with distinction.

Work Experience

Since October 2019: Tomas Bata University in Zlín, Faculty of Logistics and Crisis Management, Studentské nám 1532, 686 01 Uherské Hradiště, the Czech Republic, position:

- *assistant*: teaching informatics, applied informatics for crisis management, information systems for crisis management, introduction to LaTeX,

Since October 2018: Computer Help, spol. s r.o., Blanická 553/16, 120 00 Praha 2 - Vinohrady, the Czech Republic, position:

- *IT Administrator* (contract of employment): maintenance of the infrastructure, hardware and software support,

September 2016 – September 2018: Orange Tree s.r.o., Zelný trh 332/12, 602 00 Brno, the Czech Republic, position:

- *IT Administrator* (contract of employment): maintenance of the infrastructure, hardware and software support,

September 2016 – August 2017: Tomas Bata University in Zlín, Faculty of Applied Informatics, Nad Stráněmi 4511, 760 05, 760 01 Zlín, the Czech Republic, position:

- *assistant* (part-time): teaching mobile technologies, object-oriented programming and software used in development,

February 2013 – December 2013: EVC Group s.r.o., Nádražní 804, 768 24 Hulín, the Czech Republic, position:

- *software engineer, PHP/C++* (contract of employment): server service for automatised electromobile service mail processing,

Since January 2013: Edhouse s.r.o., Nad Stráněmi 5656, 760 05 Zlín, the Czech Republic, position:

- *software engineer, C/C++/C#* (part-time): Software development (software for testing new hardware boards used in FEI company and Thermo Fisher Scientific Inc. afterwards, static code analysis and maintenance),

November 2012 – September 2019): Tomas Bata University in Zlín, nám. T. G. Masaryka 5555, 760 01 Zlín, the Czech Republic, position:

- *young researcher* (part-time) working in The Centre for Security, Information and Advanced Technologies (CEBIA-Tech),

February 2006 – June 2011: Brno University of Technology, Faculty of Information Technology, Božetěchova 2, 612 66 Brno, the Czech Republic, position:

- *young researcher*: development of speech processing technologies.

Language Skills

- English: C1,

- German: A2,

- French: A2.

Technological Skills

- C/C++/C#, Pascal, Object Pascal (Delphi), Java, BASH, Assembler, Oracle (PL/SQL), Matlab, HTML, CSS, XML, PHP, MySQL, JavaScript,

- MS Windows and Linux operating systems (certificates: 72-270 and 72-290),

- networking (Cisco certificates: CCNA1 and CCNA2).

LIST OF APPENDICES

APPENDIX A: Software

APPENDIX A: SOFTWARE

The source code of the software mentioned in this doctoral thesis is enclosed on an optical compact disc (CD) together with its executable binaries for Linux as well as for Microsoft's Windows operating systems.

The structure of the content of the enclosed CD:

- `bin` – directory containing the executable files and additional helpful scripts for automatized running and statistical processing (for Microsoft's Windows Command Prompt):

    - `permittivity_linux64_release` – executable file for 64-bit Linux operating systems (compiled under Debian-derived distribution),

    - `permittivity_win64_release.exe` – executable file for 64-bit Microsoft's Windows operating systems,

    - `multirunner.bat` – script file for automatized sequential running of the permittivity estimator and generating statistics,

    - `sensitivity-analyser.bat` – script file for running the multirunner.bat with various input error levels,

- `doc` – directory containing software documentation which can be viewed by opening *doc/html/index.html*, the documentation can be automatically re/generated using Doxygen by executing (in the command line prompt or in a terminal): *cd src && doxygen permittivity.dox*,

- `src` – directory containing the source codes of the software written in C++, these source codes may be compiled in several ways, one possible way is to use the g++ compiler in the following manner (in the command line prompt or in a terminal): *g++ -O2 -Wall -pedantic -std=c++17 permittivity.cpp -o permittivity.exe*; this directory includes also Makefile what is a script file for a terminal in Linux operating systems containing instructions of how to build, clean, run, test memory allocations, generate documentation and create a zip archive of the project, and

- `info.txt` – file containing this information about the content of its directory.

Pavel Tomášek

Estimation of Material Permittivity in Free Space by Means of Inverse Problem Techniques

Řešení inverzního problému odhadu permitivity materiálu ve volném prostoru

Doctoral Thesis

Typography: Pavel Tomášek

2020